RSC Advances

PAPER

View Article Online
View Journal | View Issue

Cite this: *RSC Adv.*, 2024, **14**, 39174

A kinetic study for the estimation of riboflavin sensitized photooxidation of pyridoxine HCl using green UV-visible spectrometric and HPLC methods†

Zubair Anwar, *[a] Aisha Noreen,[a] Muneeba Usmani,[b] Zuneera Akram,[c] Muhammad Ahsan Ejaz,[a] Muhammad Ali Sheraz, [b] Sofia Ahmed,[b] Saima Zahid,[a] Saba Sabir[a] and Syed Ghulam Musharraf[d]

Riboflavin (RF) sensitized photooxidation of pyridoxine HCl (PD) in the pH range of 2.0–12.0 has been carried out under UV and visible irradiation in aerobic and anaerobic conditions. PD follows first-order kinetics in the absence and presence of RF for its photodegradation. The first-order rate constants (k_{obs}) for the photodegradation of PD in the presence of RF (0.05–0.50 × 10^{-4} M) in aerobic and anaerobic conditions range from 0.046–0.755 and 0.0089–0.755 × 10^{-2} min^{-1}, respectively. RF acts as a promoter for the photodegradation of PD and the second-order rate constants (k_2) are in the range of 0.026–1.285 and 0.004–0.128 × 10^{-2} M^{-1} min^{-1} in aerobic and anaerobic conditions, respectively. The k_2–pH profile for the photodegradation shows a slanted curve, indicating that with an increase in pH, the rate of photodegradation of PD also increases. Green UV-visible spectrometric and high-performance liquid chromatographic (HPLC) methods have been developed for the simultaneous determination of PD and RF in pure and degraded solutions. These two developed methods are statistically compared and it is found that there is no significant difference between them. We have conducted *in silico* studies to assess the formation of ground state complexes, molecular interactions, and the binding affinities of RF and PD.

Received 12th August 2024
Accepted 10th November 2024

DOI: 10.1039/d4ra05836d

rsc.li/rsc-advances

1. Introduction

When formulating liquid vitamin products, it's important to consider how each vitamin's chemical stability can be impacted by interactions with other vitamins. This is a significant factor to consider in the formulation process. This may destabilize one or more vitamins with a loss of potency and decreased bioavailability. The pH of the medium contributes significantly to minimizing the photochemical interaction between the vitamins and the choice of optimum pH for the formulation is critical. The different variables included in the stability of individual vitamins and mixtures in the liquid formulation have been discussed in several works.[1–38] However, many aspects still need to be investigated due to the complexity of the multi-component system based on several vitamins, the nature and composition of their degradation products, and the non-availability of suitable analytical methods.

Riboflavin (vitamin B_2, RF) (Fig. 1a) and pyridoxine hydrochloride (vitamin B_6, PD) (Fig. 1b) are the constituents found in the vitamin B complex supplements and multivitamin preparations.[35,39,40] PD is affected by light.[6,35,39–44] PD is prone to interacting with other vitamins, especially RF, when exposed to light,[45,46] dyes (eosin, rose Bengal, mercurochrome, methylene blue, Arurc (A and B)) have been shown to accelerate its photodecomposition in aqueous solution[47,48] and may undergo photosensitized degradation as in the case of many compounds mentioned above. Over the last many years, the photochemistry of RF has been of great interest to scientists.[26–30,38,49–58] RF is the highly photosensitive component[28–30,35,38–40,49,59–63] and degrade into several photoproducts (formylmethylflavin (FMF), lumichrome (LC), lumiflavin (LF), carboxymethylflavin (CMF), and cyclodehydroriboflavin (CDRF)) *via* different mechanisms (photoaddition, photodealkylation, photoreduction, photooxidation (Fig. 2)).[26,27,38,51,52,63–69] It is an efficient photosensitizer that forms $^1O_2$ (singlet oxygen), ROS (reactive oxygen species), and free radicals.[70–73] RF based photosensitization mechanism (type I and type II) leads to the photodegradation of drugs/

[a]*Department of Pharmaceutical Chemistry, Baqai Institute of Pharmaceutical Sciences, Baqai Medical University, Gadap Road, Super Highway, Karachi-75340, Pakistan. E-mail: zubair_ana@hotmail.com; zubair_ana@baqai.edu.pk*

[b]*Department of Pharmaceutics, Baqai Institute of Pharmaceutical Sciences, Baqai Medical University, Gadap Road, Super Highway, Karachi-75340, Pakistan*

[c]*Department of Pharmacology, Baqai Institute of Pharmaceutical Sciences, Baqai Medical University, Gadap Road, Super Highway, Karachi-75340, Pakistan*

[d]*Third World Centre for Science and Technology, H. E. J. Research Institute of Chemistry, University of Karachi, Karachi-75270, Pakistan*

† Electronic supplementary information (ESI) available. See DOI: https://doi.org/10.1039/d4ra05836d

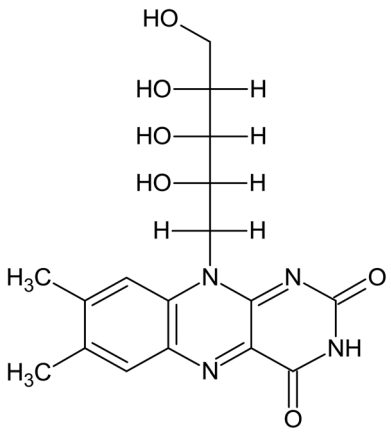

(a)

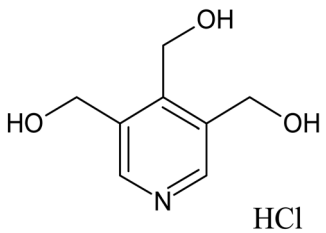

(b)

Fig. 1 Chemical structures of RF (a) and PD (b).

analytes that results in the formation of various degradation products.[72,74] RF photosensitized degradation of various drugs/substrates[63,66,71–73,75–109] has been carried out. It is important to investigate the potential negative effects of RF (a component of vitamin B-complex and multivitamin preparations) on other vitamins, as RF has photosensitization properties. However, the RF photosensitized degradation of PD at pH 2.0–12.0 in aerobic and anaerobic conditions has not been carried out. Therefore, the present study aims to determine the effect of RF and its concentrations on the photodegradation of PD and this process was carried out within a pH range of 2.0–12.0 while exposing it to UV and visible light in aerobic and anaerobic conditions. *In silico* studies have also been carried out to evaluate the molecular interaction between RF and PD to determine the binding affinity and complex formation at ground state. The UV-visible spectrometric and HPLC methods have been developed and validated using ICH guidelines[110] to simultaneously determine RF and PD in pure and degraded solutions. Also, the greenness of the proposed methods has been evaluated using the National Environmental Method Index (NEMI), an analytical eco-scale, green analytical procedure index (GAPI) and an analytical greenness (AGREE) calculator. These developed and validated methods are statistically compared for accuracy, precision and reproducibility evaluation in a mixture. This study also gives an idea of the maximum stability of PD in the presence of RF at optimum pH in multivitamin preparations. Also, the mechanisms of PD photooxidative degradation in the absence and presence of RF in aerobic and anaerobic conditions are proposed. The study would highlight the problem associated with the stability of PD in the presence of RF for the formulator to formulate stable multivitamin preparations.

2. Materials and methods

2.1 Materials

RF (99%) and PD (99%) have been obtained from Sigma-Aldrich (St. Louis, USA). All the solvents utilized in this study were of HPLC grade and were acquired from Merck & Co. (White House Station), NJ, USA. The deionized water was prepared using the Millipore-Q Plus system (Bedford, USA) and used throughout the study. The Millipore filtration assembly has been used for the filtering of solutions and solvents. The buffer systems employed in this study are given below, and the ionic strength in each case was 0.002 M.

KCl–HCl (pH 1.0–2.0)

Citric acid–Na_2HPO_4 (pH 2.5–8.0)

$Na_2B_4O_7$–HCl (pH 8.5–9.0)

$Na_2B_4O_7$–NaOH (pH 9.5–10.5)

Na_2HPO_4–NaOH (pH 11.0–12.0)

2.2 Precautions

Fresh solutions of RF and PD were employed throughout the study and were prepared in the dark to inhibit any photochemical and chemical changes. The photolysis was conducted under subdued light.

2.3 Methods

2.3.1 FTIR spectroscopy. The purity of RF and PD was determined using the Nicolet iS5 FTIR spectrophotometer with ZnSE0 windows (Thermo Fisher Scientific, USA). The RF and PD samples were placed on diamond ATR crystal (iD7ATR, Thermo Fisher Scientific, Great Britain) to collect spectra after performing 156 scans in the 4000 to 700 cm^{-1} range. The spectra obtained were analyzed using built-in Omnic software (Version 9.0).

2.3.2 Differential scanning calorimetry (DSC). The RF and PD purity was further confirmed by differential scanning calorimetry (Model DSC 100, lab kits, Hong Kong). DSC instrument was calibrated utilizing the standard indium and zinc. RF and PD were weighed (5.0 ± 0.5 mg) in the pans of aluminum, and heating was carried out at 10 °C min^{-1}, under the nitrogen flow (20 ml min^{-1}) between temperatures 30 and 400 °C.

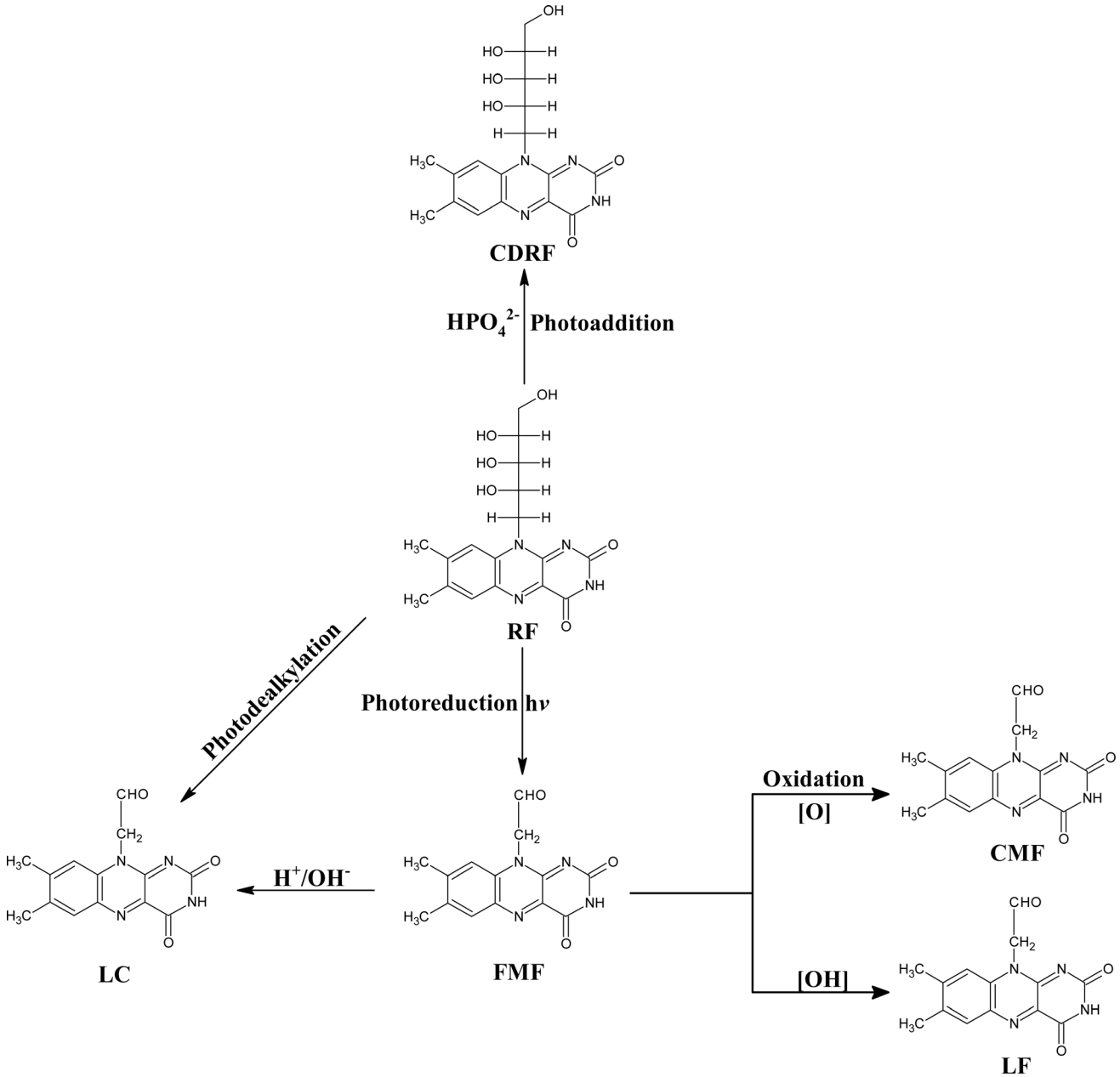

Fig. 2 Photodegradation of RF follows different degradation pathways, resulting in the formation of various photoproducts: FMF (formylmethylflavin), LC (lumichrome), LF (lumiflavin), CMF (carboxymethylflavin), CDRF (cyclodehydroriboflavin).

2.3.3 Thin layer chromatography (TLC). TLC of the pure and photodegraded RF and PD solutions was conducted. The TLC plates pre-coated with 250 μm silica gel (GF 254, Merck) were used. The solvents employed are water : acetic acid : 1-butanol : 1-propanol (18 : 2 : 50 : 30, v/v)[111] and glacial acetic acid : acetone : methanol : benzene (5 : 5 : 20 : 20, v/v)[112] for RF and PD, respectively. The 254 nm of UV-itech Comp (UK) was used to detect PD and RF.

2.3.4 UV-visible spectrometry. The spectral measurements of pure and degraded RF and PD solutions have been conducted on a UV Visible Spectrophotometer (Thermo Scientific, Evolution 201, USA) in quartz cells of path length 10 mm.

2.3.5 Light intensity determination. The light intensities of Philips TUV 36 W light and HPLN 125 W lamp were determined using the potassium ferrioxalate actinometry,[113] and the values were found to be $2.29 \pm 0.12 \times 10^{17}$ and $5.56 \pm 0.41 \times 10^{18}$ q s^{-1}, respectively. The UV lamp used in this study shows maximum emission at 270 nm and minimum at 319, 375, 405, 494, 555, and 578 nm (Fig. S1a†). Whereas, visible lamp shows maximum emission at 340, 360, 395, 490, 555, 590, 620, and 700 nm and minimum emission at 580 and 700 nm (Fig. S1b†).

2.3.6 Quantum yield determination. The quantum yields (Φ) of the photodegradation of PD in RF's presence (5.0×10^{-5} M) were calculated by the light intensity (Q) values of Philips

TUV and HPLN lamp. The area under the bands of emission of TUV and HPLN lamp absorbed by PD to the total area of the bands of emission of TUV and HPLN lamp gives Φ.

$$\Phi = \frac{\text{rate of photolysis (PD)(moles per s)} \times \text{no. of molecules/mole}}{Q} \quad (1)$$

2.3.7 Spectrometric assay method. The concentrations of PD have been determined in the presence of RF at 323 nm (pH 7.0, 0.002 M) by developing and validating a two-component spectrometric method using International Council on Harmonization (ICH) guidelines.[110] In a volumetric flask (Pyrex), 1 ml of the pure or photolyzed solution was poured into which phosphate buffer (pH 7.0, 0.002 M) was added to make up the final volume and was subjected to the spectrometric assay.

2.3.8 HPLC assay procedure. The HPLC assay procedure for the concurrent estimation of PD and RF has been developed using the HPLC system (Model LC10 ADVP, Shimadzu, Japan) was equipped with a PDA detector (Model SPD-10A VP) and controller (Model SCL-10AVP) that was connected to a microcomputer system. An octadecylsilane column with 5 μ thickness and 250 × 4.6 mm acquired from Welch, Zhejiang, China, was used for the assay procedure. The assay was conducted at room temperature (25 ± 2 °C) in an isocratic system. An acetonitrile : water (20 : 80, v/v, pH 3.5) solvent system was employed for the assay at a 1.0 ml min^{-1} flow rate. The detection was conducted at a wavelength of 280 nm. The injection volume was 20 μl using a glass syringe, and the assay procedure was validated using the guidelines of ICH.[110]

2.3.9 Photolysis. PD (1.00×10^{-4} M) solutions were prepared with and without RF ($0.10–0.50 \times 10^{-4}$ M) between pH 2.0 and 12.0 in 100 ml volumetric flask. The bubbling of air and nitrogen maintained the aerobic and anaerobic conditions for 30 minutes, respectively. Afterward, these solutions were placed in UV[63,114] (Fig. S2†) and visible irradiation[63,115] (Fig. S3†) chambers. The temperature was maintained at 25 ± 2 °C by placing the flask in the water bath. The control solution of PD subjected to conditions has been kept in the dark to estimate the air-prone oxidation of PD. The samples were withdrawn and subjected to TLC, spectrometric, and HPLC analysis at appropriate intervals.

2.3.10 Assay method validation. The validation of the two-component spectrometric and HPLC assay method for the simultaneous analysis of PD and RF was conducted using ICH guidelines.[110] The studied parameters include system suitability, linearity, accuracy, precision, limit of detection (LOD), and limit of quantification (LOQ). The details of the assay method validation are given in the ESI.†

2.3.11 Statistical evaluation. The proposed UV-visible spectrometric and HPLC methods were statistically compared using Statistical Analysis in Social Sciences Software (SPSS, version 25.0).

2.3.12 *In silico* studies. *In silico* studies have been carried out to evaluate the molecular interaction between PD and RF and the formation of the ground state complex. Also, the binding affinity (kcal mol^{-1}) between PD and RF has been evaluated to determine how strongly they are bound together. The structure of PD and RF has been obtained from PubChem and Biovia Discovery Studio was used to evaluate the molecular interaction, formation of ground state complex and binding affinity. The PD was docked with RF to complete the interactions using Pyrx virtual screening software.

2.3.13 Total organic carbon (TOC) analysis. The mineralization of PD, RF, and RF–PD has been determined to evaluate the extent of the degradation using a Sievers 500 RL on-line TOC analyzer. The analysis was carried out before and after carrying out irradiation under visible light (pH 7.0) for 2 h to determine the final TOC content in the samples.

3. Results and discussion

3.1 Purity confirmation

Purity determination is an important consideration before carrying out the validation of assay methods and degradation studies. So, therefore, FTIR and DSC studies were conducted to assess the purity of RF and PD used in the proposed study.

Chemically, PD is 4,5-bis(hydroxy methyl)-2-methyl pyridine-3-ol-hydrochloride, and its FTIR spectrum is given in Fig. S4.† The characteristic peaks at 3233, 2975, 1827, 1731, 1600–1400, 1300, and 1012–1004 cm^{-1} correspond to OH vibrations, C–H stretching, C–H stretching, C–OH stretching, C–C aromatic ring stretching vibrations, C–O stretching vibrations and C–OH attaches to pyridine ring, respectively.[116–118] The FTIR spectrum of RF (7,8-dimethyl-10-[(2*S*,3*S*,4*R*)-2,3,4,5 tetrahydroxy pentyl] benzo[*g*]pteridine-2,4-dione) is given in Fig. S4.† RF shows characteristic peaks at 3370, 1650, 1580, 1550, and 1150 cm^{-1} correspond to OH/NH, C=O, C=C, C=N, C–OH, and ribose moiety, respectively.[43,63] The obtained spectra of RF and PD were compared with those given in the literature, and it has been found that the materials used are pure and could be used for the method validation and degradation studies.

DSC further ascertained the purity of PD and RF. PD shows an endothermic peak at 159.8 °C (Fig. S5†), as reported earlier.[119] However, RF decomposes at 280 °C and shows no endothermic peak.[43,63] The results indicate that the samples used are pure and can be used to validate assay methods and decomposition studies.

3.2 Spectral characteristics of PD alone and PD in the presence of RF

The absorption maxima of PD and RF at pH 2.0, 4.5, 7.0, and 9.0 have been determined. It has been found that PD shows absorption maxima at 290, 290 and 323, 223, 254 and 323, and 290 nm at pH 2.0, 4.5, 7.0, and 9.0, respectively (Fig. 3). PD possesses the pK_a values of 5, 9, and 15.[120] The spectrum of PD at pH 2.0 shows an absorption maximum at 290 nm, which is due to the N_1/O_3 protonated species, whereas the spectrum at pH 4.5 corresponds to the mixture of neutral and N_1 protonated form of PD showing absorption maxima at 290 and 323 nm. However, at pH 7.0, PD shows absorption maxima at 223, 254, and

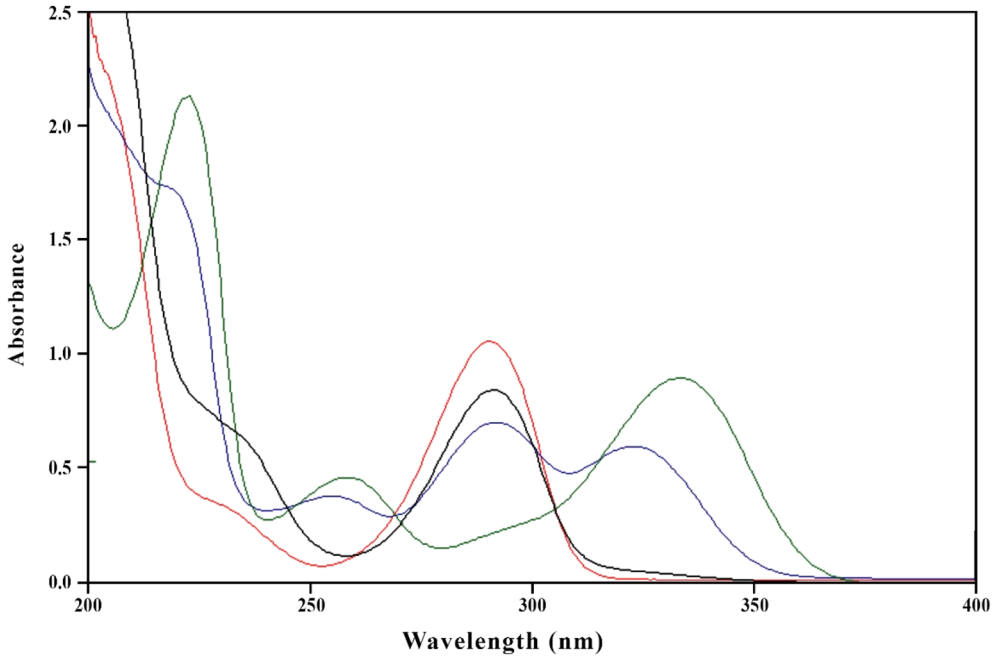

Fig. 3 Absorption spectra of PD (1.00×10^{-4} M) in aqueous solution at pH 2.0 (red line), 4.5 (blue line), 7.0 (green line) and 9.0 (black line).

323 nm, which is due to the neutral O_3 hydroxyl or zwitterionic or oxo species. At pH 11.0, PD shows absorption maxima at 290 nm, which is due to the N_1/O_3 deprotonated form of PD.[121] The PD is a UV-absorbing drug that shows absorption maxima at 254 and 323 nm (pH 7.0) (Fig. 3). However, RF shows absorption maxima at 223, 267, 374, and 444 nm.[39,63] The absorption spectra of RF (0.50×10^{-4} M) and PD (1.00×10^{-4} M) at pH 2.0, 4.5, 7.0, and 9.0 are given in Fig. S6a and b.† Two-component spectrometric assay method for the simultaneous determination of RF and PD in pure and degraded solutions has been developed and validated at pH 7.0 using ICH guidelines,[110] as there is a considerable difference in the absorption maxima of both.

3.3 *In silico* studies

The molecular interaction, binding affinity and formation of ground state complex between PD and RF have been determined by *in silico* studies. This indicates that there is molecular interaction between RF and PD with a binding affinity of -2.9 kcal mol^{-1}, which results in the formation of a ground state complex (Fig. S7†). PD and RF *in silico* docking studies show that there are hydrophobic linkages (alkyl and π-alkyl) between carbon and hydrogen atoms. The loss of one hydrogen from the methyl group of PD and RF leads to the formation of the bond between them with a bond length of 4.11 Å. Also, there are some hydrophobic linkages between the methyl group of PD and RF with bond lengths of 4.04 and 5.14 Å.

3.4 Assay methods

3.4.1 Simultaneous two-component spectrometric assay method. The absorption maxima of PD and RF are 290, 223, 254, 323 (ref. 121) and 223, 267, 385, and 445 nm, respectively (Fig. S5a and b†).[39,40] However, at pH 7.0 the absorption maxima of PD and RF are 223, 254, and 323 and 223, 267, 385, and 445 nm, so, therefore, pH 7.0 has been selected for the development and validation of a two-component spectrometric assay of PD and RF (Fig. S5b†). The simultaneous determination of PD and RF using a two-component spectrometric method (pH 7.0) has been validated according to the ICH guidelines[110] and the validation data are reported in Table 1. The proposed method is linear in the concentration range of 0.05–0.50 $\times 10^{-4}$ M and 0.50–1.00 $\times 10^{-4}$ M for RF and PD, respectively (Fig. S8a†). The accuracy and precision of the proposed method

Table 1 Calibration data of the two-component spectrometric method for the simultaneous determination of pyridoxine (PD) and riboflavin (RF) in an aqueous solution at pH 7.0

	PD	RF
λ_{max}, nm	323	385
Linearity		
Range ($M \times 10^4$)	0.10–1.00	0.05–0.50
Correlation coefficient	0.9997	0.9998
Slope ($M \times 10^3$)	9.37	9.03
SE of slope[a] ($M \times 10^3$)	6.89	2.55
Intercept ($\times 10^2$)	1.09	0.37
SE of intercept[b] ($\times 10^3$)	4.70	2.24
SD of intercept[c] ($\times 10^3$)	14.9	7.09
Mean accuracy (%) ± SD	99.39 ± 0.96	99.74 ± 1.13
Precision (% RSD)	0.97	1.14
LOD[d] ($M \times 10^5$)	0.52	0.26
LOQ[e] ($M \times 10^5$)	1.59	0.78

[a] Standard error of slope. [b] Standard error of intercept. [c] Standard deviation of the intercept. [d] Limit of detection. [e] Limit of quantification.

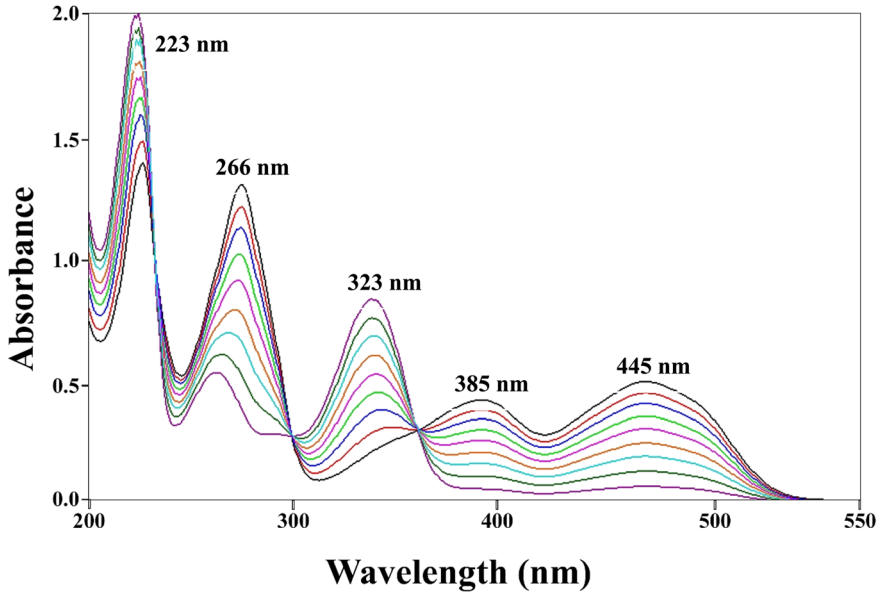

Fig. 4 Overlay absorption spectra of PD (0.10–0.90 × 10^{-4} M) and RF (0.05–0.50 × 10^{-4} M) at pH 7.0 of the synthetic mixture, where 223, 266, 385, 445 and 323 nm correspond to the absorption maxima of RF and PD, respectively.

to determine the PD and RF are found to be in the range of 100.3–100.7%, 99.70–100.2%, and 0.29–0.48%, 0.30–0.55%, respectively (Tables S1 and S2†). So, therefore, the developed method can be used for the determination of PD and RF in pure and degraded solutions. This method has been applied to the synthetic mixture of PD and RF to evaluate the accuracy, precision, reliability, and reproducibility of the proposed method (Fig. 4) and the results obtained are given in Table S3.†

3.4.2 HPLC assay method. The HPLC method for simultaneous determination of PD and RF in an aqueous solution (at pH 3.5) has been developed and validated according to the ICH guidelines.[110] RF (0.50 × 10^{-4} M) and PD (1.00 × 10^{-4} M) chromatograms for their simultaneous determination are given in Fig. 5. The proposed HPLC method is found to be linear in the concentration range of 0.05–0.50 × 10^{-4} and 0.10–1.00 × 10^{-4} M for RF and PD, respectively (Fig. S8b†). A statistical

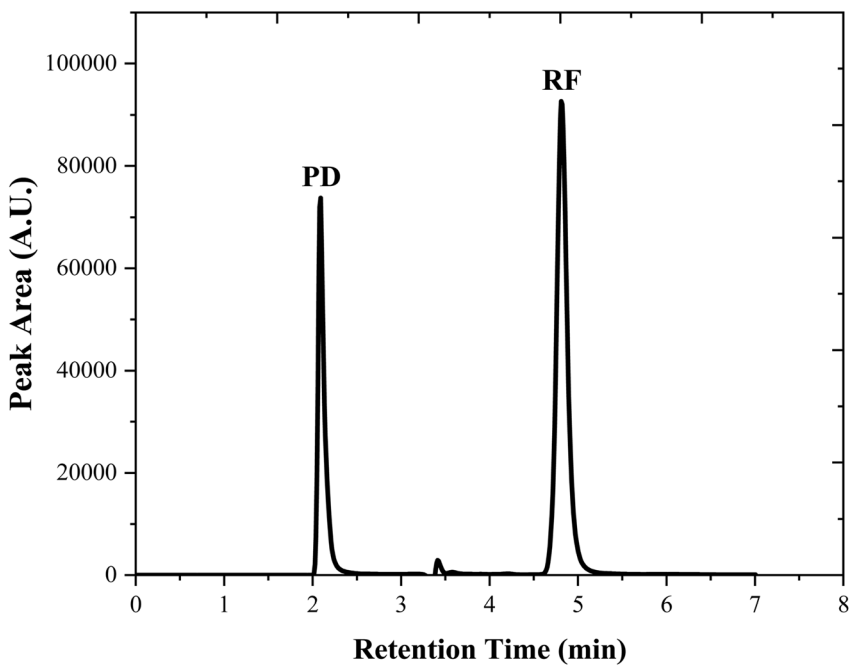

Fig. 5 Chromatograms of PD (1.00 × 10^{-4} M) and RF (0.50 × 10^{-4} M) in an aqueous solution (pH 3.50) at room temperature (25 ± 2 °C) and the retention time are 2.10 and 4.8 min for PD and RF, respectively.

Table 2 Calibration data of the HPLC method for the determination of pyridoxine (PD) and riboflavin (RF) in an aqueous solution at pH 3.5

	PD	RF
λ_{max}, nm	280	280
Retention time (t_R), min	2.10	4.81
RSD (%)	0.58	0.66
N^a	9450	8800
T^b	0.77	0.65
Linearity		
Range (M × 10^4)	0.10–1.00	0.05–0.50
Correlation coefficient	0.9999	0.9999
Slope (M × 10^9)	5.74	24.9
SE of slope^c (M × 10^3)	2.40	3.35
Intercept (×10^3)	2.16	10.9
SE of intercept^d (×10^3)	2.65	2.29
SD of intercept^e (×10^3)	8.38	7.23
Mean accuracy (%) ± SD	99.95 ± 0.73	100.1 ± 0.84
Precision (% RSD)	0.73	0.84
LOD^f (M × 10^5)	0.480	0.096
LOQ^g (M × 10^5)	1.460	0.290

^{a} Theoretical plates. ^{b} Tailing factor. ^{c} Standard error of slope. ^{d} Standard error of intercept. ^{e} Standard deviation of the intercept. ^{f} Limit of detection. ^{g} Limit of quantification.

evaluation has been carried out to determine the linearity parameters and is given in Table 2. The accuracy and precision of the HPLC method are given in Tables S4 and S5† and found that the proposed method is accurate ((100.3–101.01%, PD), (98.9–101.0%, RF)) and precise ((0.52–0.53% RSD, PD), (0.29–0.92% RSD, RF)). The proposed HPLC method is found to be robust for the simultaneous determination of PD and RF (Table S6†) by applying deliberate changes. The designed HPLC method has been applied to the synthetic mixtures of PD and RF to evaluate the method's accuracy ((99.74–101.4%, PD), (99.51–100.8%, RF)) and precision ((0.17–0.87% RSD, PD), (0.18–0.99% RSD, RF)) (Table S7†). The two developed methods are statistically compared by applying a student *t*-test for the determination of PD (0.10–1.00 × 10^{-4} M) in an aqueous solution (Table 3). The *t*-calculated value is −0.22 with a *p*-value of 0.827 which is greater than 0.05, indicating that there is no significant difference between the two developed assay methods for the estimation of PD in pure and degraded solutions. Therefore, the results obtained from both methods for the determination of PD are accurate, precise, reliable, and comparable.

3.4.3 Greenness evaluation of the developed methods. Several green assessment tools are reported in the literature,[122] to evaluate the greenness of the developed methods. The evaluation of the greenness of the method is dependent on the extent of hazardous and corrosive materials used, the waste materials produced, and the chemicals accumulated in the environment.[123,124] The greenness of the developed two-component spectrometric and HPLC methods for simultaneously determining PD and RF has been estimated using four green assessment tools including NEMI, analytical eco-scale, GAPI, and AGREE calculator.

The pictogram of the NEMI illustration to evaluate the greenness of the method is given in Fig. 6a and b. This four-quadrant pictogram indicates the use of persistent, bio-accumulative, and toxic (PBT) materials, unsafe chemicals, corrosive and waste materials (>50 g) generated. The pictogram obtained shows that the two-component spectrometric method is said to be a green method because all quadrants are green (Fig. 6a). However, the HPLC method is found to be considerably green with three out of four quadrants being green (PBT, corrosive, wastage) and one being yellow (hazardous) which is due to the use of acetonitrile in the mobile phase (20 ml/100 ml) (Fig. 6b).

Another tool for evaluating the greenness of these proposed methods is an analytical eco-scale depending on the penalty points (PPs) given for using hazardous material, energy consumption, amount of reagents used, and waste material produced[125] (>75 = excellent green, 50–75 = considerably green, <50 = not green). The analytical eco-scale score of the developed methods has been calculated by subtracting the penalty points obtained from the total value (100). The points obtained for the two-component spectrometric and HPLC method are 06 and 19 with an overall score of 94.0 and 81.0, respectively (Table 4), indicating that the methods are green as mentioned in Globally

Table 3 Comparative analysis for the determination of PD (0.10–1.00 × 10^4 M) using HPLC and UV method

HPLC				UV		
Added (M × 10^4)	Found^a (M × 10^4)	Recovery (%)	RSD (%)	Found^a (M × 10^4)	Recovery (%)	RSD (%)
0.100	0.100	100.0	0.22	0.099	99.00	0.41
0.200	0.199	99.50	0.36	0.199	99.50	0.39
0.300	0.301	100.3	0.49	0.302	100.7	0.22
0.400	0.400	100.0	0.11	0.403	100.7	0.51
0.500	0.503	100.6	0.63	0.506	101.2	0.63
0.600	0.601	100.2	0.29	0.601	100.2	0.44
0.700	0.703	100.4	0.44	0.703	100.4	0.19
0.800	0.806	100.7	0.63	0.810	101.2	0.85
0.900	0.904	100.4	0.72	0.909	101.0	0.63
1.000	1.010	101.0	0.63	0.998	99.80	0.73

^{a} Values represent the mean of 5 determinations. The calculated *t*-value is −0.22 with a *p*-value of 0.827 which is greater than the *p*-value (0.05) at a 95% confidence level indicating that the results obtained from the proposed methods have no significant difference.

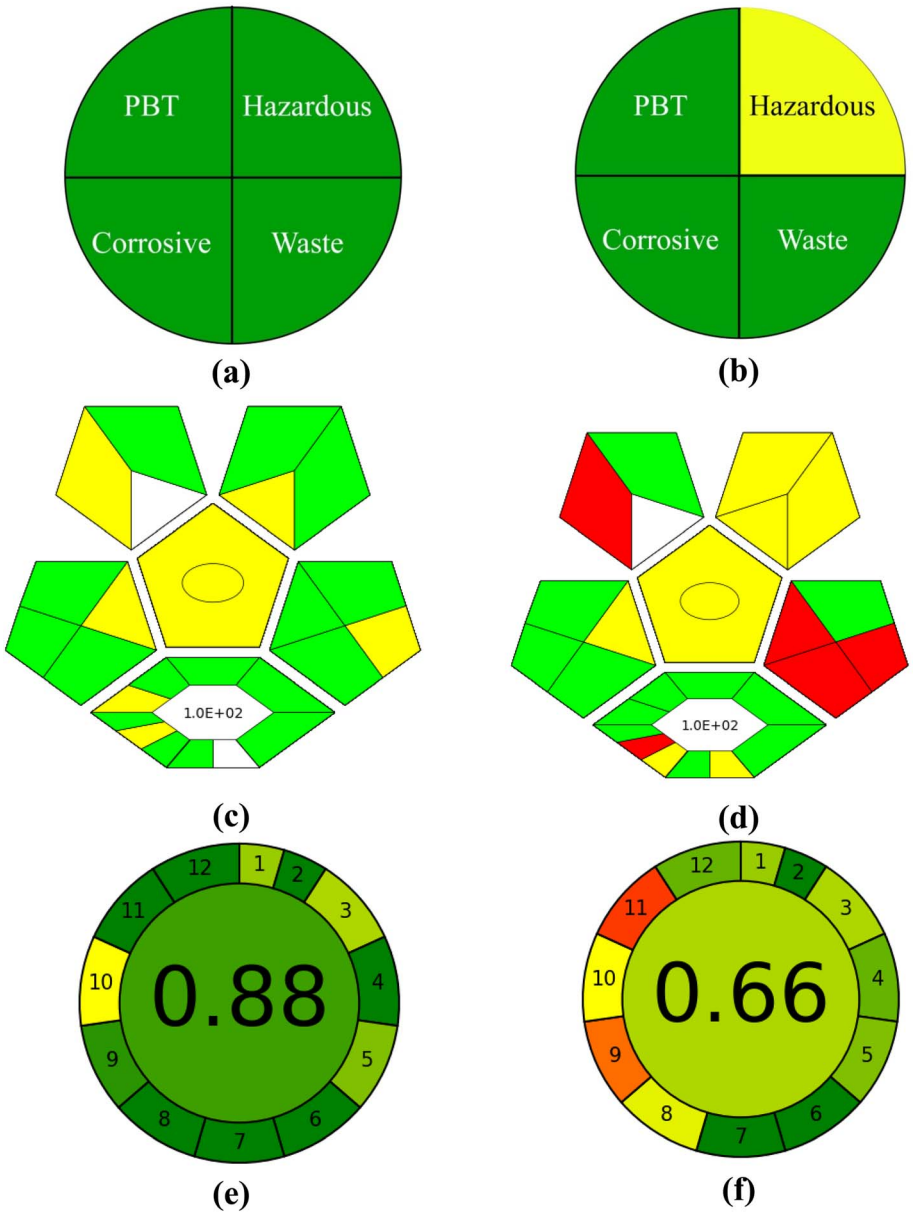

Fig. 6 NEMI (a and b), GAPI (c and d), and AGREE (e and f) analysis for the estimation of the developed UV-vis spectroscopic and HPLC methods.

Table 4 The penalty points for the determination of UV-visible spectrometry and HPLC methods

	Penalty points	
	UV-vis spectroscopy	HPLC
Citro-phosphate buffer (pH 7.0, 0.002 M)	0.00	0.00
Acetonitrile	—	6.00
Instrument energy consumption (kW h)	1.00	2.00
Sonicator	0.00	0.00
Occupational hazards	0.00	6.00
Waste (>10.0 ml)	5.00	5.00
Totally penalty points	6.00	19.0
Analytical eco-scale score[a]	94.0	81.0

[a] If analytical eco-scale score is >75 = excellent green, 50–75 = considerably green and <50 = not green.

Harmonized System of Classification and Labelling of Chemicals.[126]

The green analytical procedure index (GAPI) estimated the method's greenness by a pictogram with 15 subsections with a green, yellow, and red color indicating the excellent green, considerably green and nongreen methods.[127] The pictograms obtained for these two methods are given in Fig. 6(c and d) indicating that the two-component spectrometric method is green whereas the HPLC method is considerably green.[128,129]

The AGREE calculator is based on the 12 parameters and gives a cumulative score. A score of 1.0 shows the method is excellent green, however, if the score is less than 0.60 then the method is said to be non-green. The figure obtained for the two-component spectrometric and HPLC assay methods are given in Fig. 6e and f, with a cumulative score of 0.88 (Fig. 6e) and 0.66

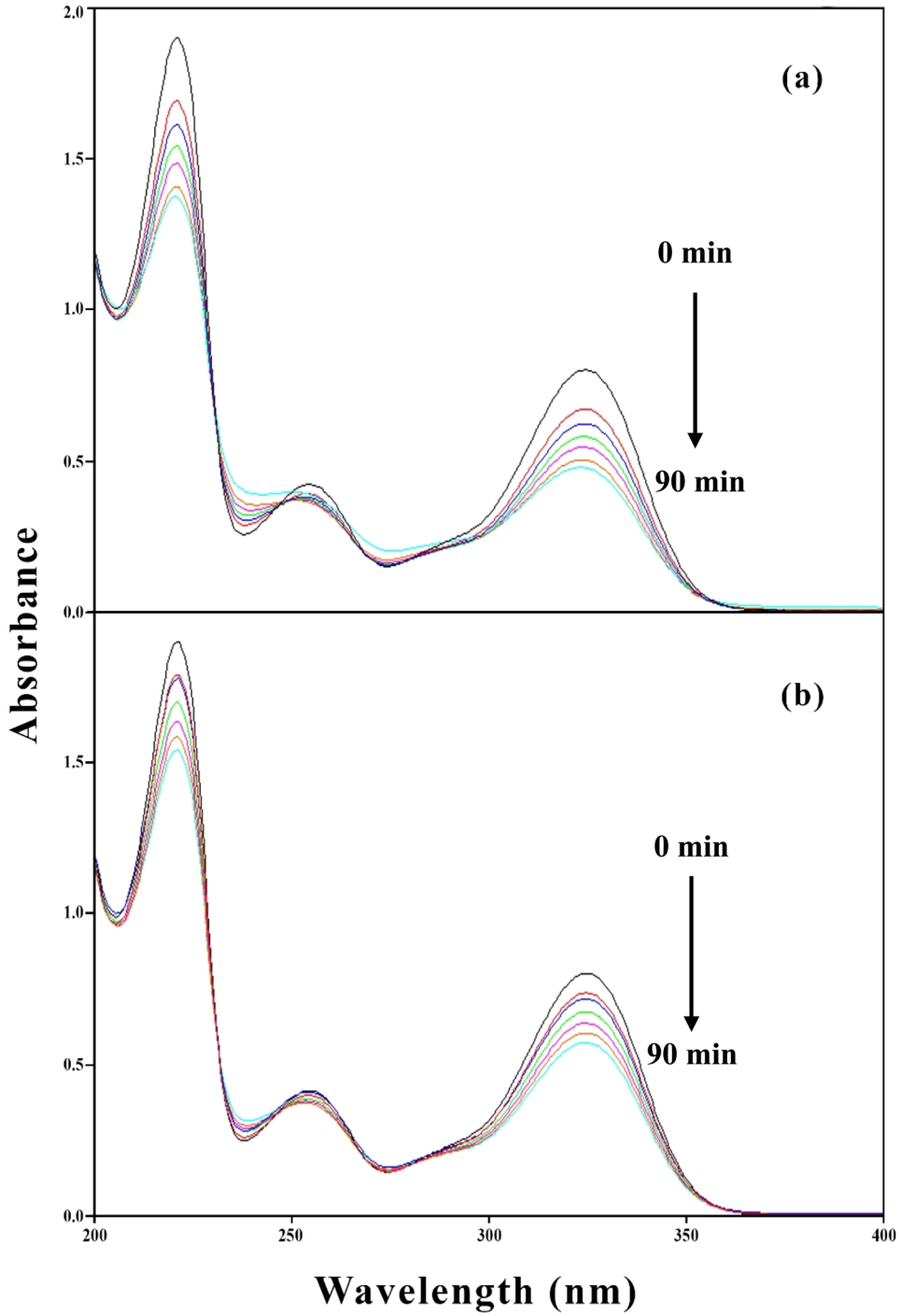

Fig. 7 Overlay spectra of PD (1.00×10^{-4} M) on photolysis at pH 7.0 using UV (a) and visible irradiation (b) sources.

(Fig. 6f), respectively, indicating that the two-component spectrometric method is excellent green (0.88) whereas the HPLC method is considerably green (0.66).

3.5 Spectral variations of photolyzed solutions of PD

PD possesses different ionic (cationic, dipolar, neutral, anionic) species at different pH values[121] due to which it shows absorption maxima at 290, 290 and 323, 223, 254, 323, and 290 nm at pH 2.0, 4.5, 7.0, and 9.0, respectively. The overlay spectra for the PD photolysis at pH 7.0 under UV and visible irradiation are given in Fig. 7a and b, respectively. The spectral changes that occur in UV irradiation are greater as compared to those of visible irradiation (Fig. 7a). The greater loss of absorbance in UV irradiation is due to the maximum emission of light at 254 nm and minimum at 324 nm, which is like the absorption maxima of PD, which is 254 nm. However, the visible light used in this study emits light at 350 and higher, resulting in the minimum

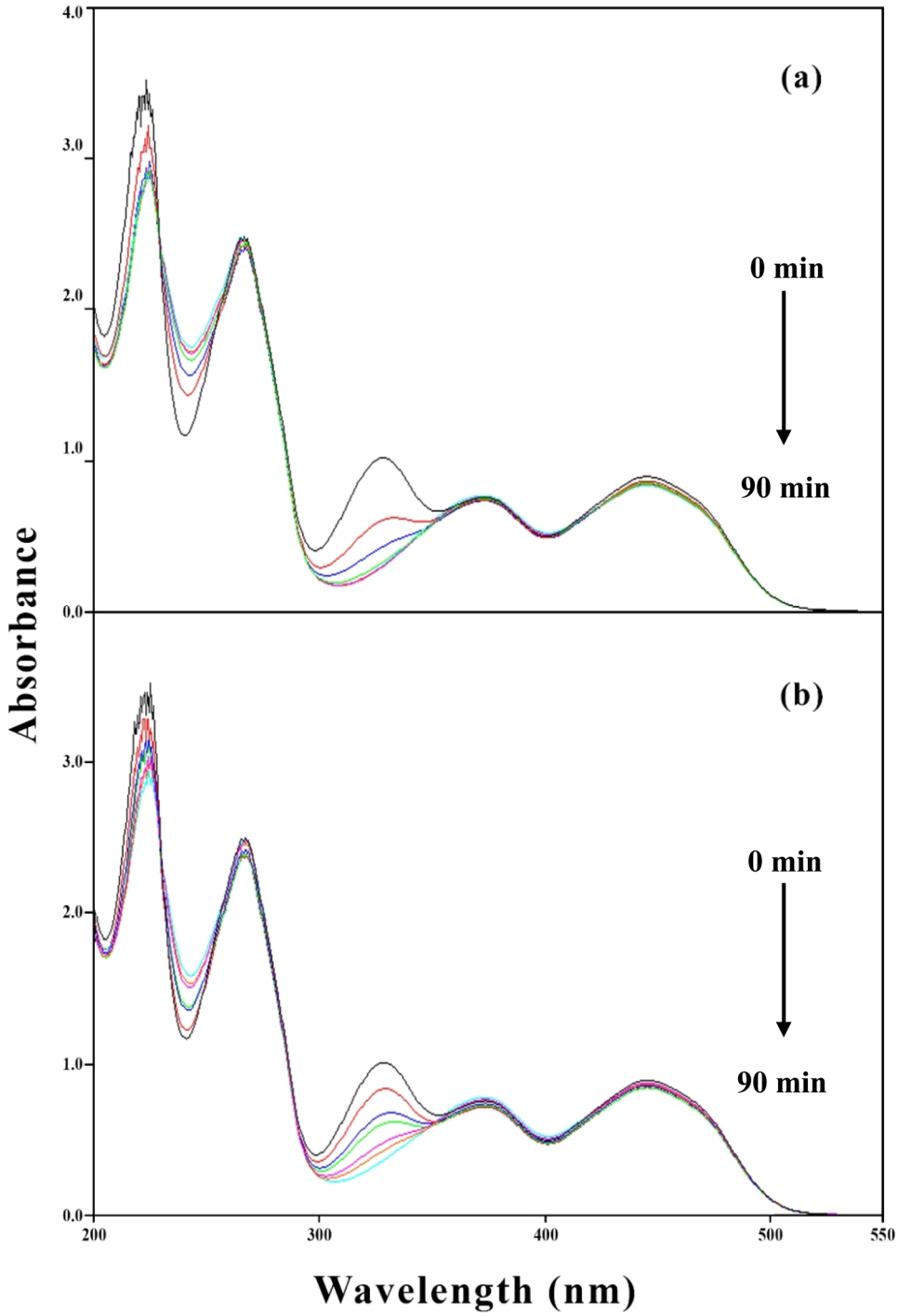

Fig. 8 Overlay spectra of PD (1.00×10^{-4} M) in the presence of RF (5.00×10^{-5} M) in visible (a) and UV (b) irradiation sources.

light absorption by PD molecules and less degradation (Fig. 7b). The overlay absorption spectra of PD (1.00×10^{-4} M) in the presence of RF (0.50×10^{-4} M) at pH 7.0 after UV and visible irradiation are given in Fig. 8a and b, respectively. RF shows absorption maxima at 223, 267, 385, and 445 nm at pH 7.0, the latter two bands are responsible for the photosensitized degradation of substrates and drugs.[63] In the presence of RF, the loss of absorbance at 323 nm, corresponds to the absorption maxima of PD, which is greater under visible radiation as compared to that of UV irradiation. This is due to the greater absorption of visible light by RF (>350 nm), which corresponds to its absorption maxima (385 and 445 nm) that results in the increased RF-sensitized degradation of PD. However, the less absorbance change at 325 nm (PD) in the presence of RF in UV irradiation is due to the less absorption of light by RF as UV light maximum emission occurs at 254 nm and less at 385 and

Table 5 First-order rate constants (k_{obs}) for the photolysis of PD in the presence of RF and second-order rate constants (k_2) for the photochemical interaction of PD with RF at pH 2.0–12.0 in aerobic conditions

		Visible light				UV light			
pH	Concentration of RF ($M \times 10^4$)	$k_{obs} \times 10^2$ (min^{-1}) ± SD[a]	$k_0 \times 10^2$ (min^{-1})	$k_2 \times 10^2$ (M^{-1} min^{-1})	Φ^b	$k_{obs} \times 10^2$ (min^{-1}) ± SD[a]	$k_0 \times 10^2$ (min^{-1})	$k_2 \times 10^2$ (M^{-1} min^{-1})	Φ^b
2	0.1	0.112 ± 0.15	0.050	0.069	—	0.046 ± 0.11	0.020	0.026	—
	0.2	0.192 ± 0.11			—	0.075 ± 0.23			—
	0.3	0.258 ± 0.23			—	0.101 ± 0.45			—
	0.4	0.317 ± 0.13			—	0.124 ± 0.33			—
	0.5	0.388 ± 0.26			0.467	0.152 ± 0.25			0.108
3	0.1	0.122 ± 0.35	0.070	0.071	—	0.048 ± 0.11	0.022	0.027	—
	0.2	0.197 ± 0.11			—	0.077 ± 0.61			—
	0.3	0.268 ± 0.75			—	0.105 ± 0.72			—
	0.4	0.330 ± 0.25			—	0.129 ± 0.27			—
	0.5	0.399 ± 0.45			0.480	0.156 ± 0.41			0.111
4	0.1	0.133 ± 0.55	0.075	0.077	—	0.052 ± 0.73	0.024	0.029	—
	0.2	0.209 ± 0.11			—	0.082 ± 0.65			—
	0.3	0.281 ± 0.22			—	0.110 ± 0.19			—
	0.4	0.361 ± 0.25			—	0.141 ± 0.22			—
	0.5	0.433 ± 0.36			0.521	0.169 ± 0.63			0.120
5	0.1	0.151 ± 0.46	0.087	0.090	—	0.059 ± 0.11	0.026	0.034	—
	0.2	0.240 ± 0.75			—	0.094 ± 0.15			—
	0.3	0.327 ± 0.11			—	0.128 ± 0.19			—
	0.4	0.407 ± 0.26			—	0.159 ± 0.26			—
	0.5	0.499 ± 0.11			0.601	0.195 ± 0.25			0.139
6	0.1	0.240 ± 0.45	0.110	0.129	—	0.094 ± 0.24	0.044	0.050	—
	0.2	0.373 ± 0.63			—	0.146 ± 0.21			—
	0.3	0.496 ± 0.46			—	0.194 ± 0.45			—
	0.4	0.629 ± 0.31			—	0.246 ± 0.63			—
	0.5	0.755 ± 0.29			0.909	0.295 ± 0.11			0.210
7	0.1	0.327 ± 0.16	0.150	0.183	—	0.128 ± 0.19	0.055	0.072	—
	0.2	0.517 ± 0.17			—	0.202 ± 0.29			—
	0.3	0.704 ± 0.22			—	0.275 ± 0.23			—
	0.4	0.890 ± 0.51			—	0.348 ± 0.45			—
	0.5	1.060 ± 0.33			1.276	0.415 ± 0.61			0.296
8	0.1	0.586 ± 0.11	0.240	0.306	—	0.229 ± 0.72	0.107	0.120	—
	0.2	0.867 ± 0.25			—	0.339 ± 0.33			—
	0.3	1.180 ± 0.36			—	0.463 ± 0.45			—
	0.4	1.502 ± 0.45			—	0.587 ± 0.51			—
	0.5	1.810 ± 0.65			1.808	0.707 ± 0.61			0.504
9	0.1	0.885 ± 0.11	0.420	0.459	—	0.346 ± 0.22	0.171	0.178	—
	0.2	1.350 ± 0.19			—	0.528 ± 0.11			—
	0.3	1.760 ± 0.22			—	0.689 ± 0.45			—
	0.4	2.265 ± 0.25			—	0.885 ± 0.33			—
	0.5	2.720 ± 0.43			3.274	1.060 ± 0.41			0.755
10	0.1	1.240 ± 0.19	0.551	0.702	—	0.485 ± 0.11	0.221	0.274	—
	0.2	1.920 ± 0.23			—	0.752 ± 0.22			—
	0.3	2.600 ± 0.41			—	0.990 ± 0.19			—
	0.4	3.340 ± 0.63			—	1.305 ± 0.31			—
	0.5	4.050 ± 0.22			4.875	1.580 ± 0.31			1.126
11	0.1	1.760 ± 0.17	0.872	1.018	—	0.689 ± 0.45	0.323	0.395	—
	0.2	2.860 ± 0.29			—	1.180 ± 0.71			—
	0.3	3.890 ± 0.11			—	1.510 ± 0.81			—
	0.4	4.821 ± 0.19			—	1.880 ± 0.11			—
	0.5	5.832 ± 0.17			7.021	2.270 ± 0.11			1.620
12	0.1	2.411 ± 0.12	1.103	1.285	—	0.945 ± 0.09	0.472	0.501	—
	0.2	3.623 ± 0.63			—	1.420 ± 0.26			—
	0.3	4.482 ± 0.45			—	1.890 ± 0.31			—
	0.4	6.190 ± 0.77			—	2.420 ± 0.42			—
	0.5	7.551 ± 0.45			9.090	2.950 ± 0.51			2.103

[a] Values represent mean of 5 determinations. [b] Quantum yield of photolysis.

Table 6 First-order rate constants (k_{obs}) for the photolysis of PD in the presence of RF and second-order rate constants (k_2) for the photochemical interaction of PD with RF at pH 2.0–12.0 in anaerobic conditions

		Visible light				UV light			
pH	Concentration of RF ($M \times 10^4$)	$k_{obs} \times 10^2$ (min^{-1}) ± SD[a]	$k_0 \times 10^2$ (min^{-1})	$k_2 \times 10^2$ (M^{-1} min^{-1})	Φ^b	$k_{obs} \times 10^2$ (min^{-1}) ± SD[a]	$k_0 \times 10^2$ (min^{-1})	$k_2 \times 10^2$ (M^{-1} min^{-1})	Φ^b
2	0.1	0.0112 ± 0.63	0.0041	0.0061	—	0.0089 ± 0.11	0.0040	0.0042	—
	0.2	0.0192 ± 0.22			—	0.0138 ± 0.45			—
	0.3	0.0260 ± 0.15			—	0.0191 ± 0.61			—
	0.4	0.0320 ± 0.11			—	0.0231 ± 0.79			—
	0.5	0.0383 ± 0.45			0.046	0.0280 ± 0.11			0.019
3	0.1	0.0122 ± 0.63	0.0053	0.0070	—	0.0090 ± 0.32	0.0049	0.0051	—
	0.2	0.0201 ± 0.45			—	0.0142 ± 0.45			—
	0.3	0.0271 ± 0.19			—	0.0184 ± 0.71			—
	0.4	0.0331 ± 0.22			—	0.0231 ± 0.86			—
	0.5	0.0392 ± 0.67			0.047	0.0270 ± 0.11			0.021
4	0.1	0.0133 ± 0.73	0.0060	0.0082	—	0.0096 ± 0.91	0.0053	0.0055	—
	0.2	0.0211 ± 0.81			—	0.0152 ± 0.26			—
	0.3	0.0281 ± 0.09			—	0.0203 ± 0.11			—
	0.4	0.0361 ± 0.22			—	0.0241 ± 0.88			—
	0.5	0.0433 ± 0.19			0.052	0.0291 ± 0.85			0.022
5	0.1	0.0151 ± 0.71	0.0065	0.0094	—	0.0112 ± 0.11	0.0061	0.0066	—
	0.2	0.0240 ± 0.45			—	0.0173 ± 0.45			—
	0.3	0.0321 ± 0.69			—	0.0236 ± 0.71			—
	0.4	0.0407 ± 0.22			—	0.0291 ± 0.23			—
	0.5	0.0499 ± 0.14			0.060	0.0361 ± 0.62			0.025
6	0.1	0.0240 ± 0.32	0.0110	0.0131	—	0.0172 ± 0.21	0.0112	0.0131	—
	0.2	0.0373 ± 0.65			—	0.0272 ± 0.71			—
	0.3	0.0496 ± 0.11			—	0.0358 ± 0.82			—
	0.4	0.0629 ± 0.22			—	0.0451 ± 0.63			—
	0.5	0.0755 ± 0.51			0.090	0.0544 ± 0.22			0.038
7	0.1	0.0327 ± 0.63	0.0150	0.0181	—	0.0231 ± 0.23	0.0148	0.0198	—
	0.2	0.0517 ± 0.71			—	0.0371 ± 0.71			—
	0.3	0.0704 ± 0.86			—	0.0508 ± 0.22			—
	0.4	0.0891 ± 0.29			—	0.0641 ± 0.51			—
	0.5	0.1061 ± 0.31			0.128	0.0773 ± 0.22			0.055
8	0.1	0.0586 ± 0.45	0.0251	0.0312	—	0.0421 ± 0.63	0.0302	0.0345	—
	0.2	0.0867 ± 0.71			—	0.0627 ± 0.71			—
	0.3	0.1181 ± 0.22			—	0.0856 ± 0.52			—
	0.4	0.1501 ± 0.71			—	0.1081 ± 0.81			—
	0.5	0.1812 ± 0.79			0.218	0.1301 ± 0.22			0.093
9	0.1	0.0885 ± 0.86	0.0422	0.0461	—	0.0641 ± 0.45	0.0421	0.0451	—
	0.2	0.1351 ± 0.11			—	0.0982 ± 0.73			—
	0.3	0.1762 ± 0.71			—	0.1273 ± 0.11			—
	0.4	0.2263 ± 0.45			—	0.1631 ± 0.45			—
	0.5	0.2720 ± 0.71			0.327	0.1961 ± 0.73			0.140
10	0.1	0.1241 ± 0.91	0.0561	0.0701	—	0.0891 ± 0.16	0.0611	0.0635	—
	0.2	0.1921 ± 0.22			—	0.1393 ± 0.22			—
	0.3	0.2604 ± 0.64			—	0.1841 ± 0.91			—
	0.4	0.3351 ± 0.48			—	0.2411 ± 0.22			—
	0.5	0.4052 ± 0.77			0.488	0.2932 ± 0.51			0.208
11	0.1	0.1763 ± 0.45	0.0811	0.1022	—	0.1271 ± 0.63	0.0911	0.0945	—
	0.2	0.2862 ± 0.22			—	0.2061 ± 0.45			—
	0.3	0.3891 ± 0.61			—	0.2791 ± 0.22			—
	0.4	0.4821 ± 0.53			—	0.3480 ± 0.11			—
	0.5	0.5832 ± 0.81			0.702	0.4211 ± 0.63			0.300
12	0.1	0.2411 ± 0.81	0.1030	0.1281	—	0.1741 ± 0.71	0.1131	0.0965	—
	0.2	0.3623 ± 0.45			—	0.2622 ± 0.22			—
	0.3	0.4484 ± 0.61			—	0.3503 ± 0.69			—
	0.4	0.6201 ± 0.86			—	0.4471 ± 0.70			—
	0.5	0.7551 ± 0.91			0.909	0.5452 ± 0.89			0.388

[a] Values represent the mean of 5 determinations. [b] Quantum yield of photolysis.

445 nm (which corresponds to RF absorption maxima) resulting in less energy transfer from RF to PD and decreased RF photosensitized degradation of PD (Fig. 8b).

3.6 Kinetics of photodegradation of PD in absence and presence of RF

The photodecomposition of PD with and without RF (0.1–1.5 × 10^{-5} M) has been carried out in aqueous solution (pH 2.0–12.0) in aerobic and anaerobic conditions. It has been found that PD follows first-order photodegradation kinetics for its degradation in the absence and presence of RF. The log concentration *versus* time (min) plots in the presence of numerous RF concentrations (0.1–1.5 × 10^{-4} M) have been plotted. The following graphs were utilized to compute the rate constants of the first order (k_{obs}) for the photodecomposition of PD using UV and visible irradiation in aerobic and anaerobic conditions. The photolysis rate constants of PD in the absence (k_0) and presence (k_{obs}) of RF in aerobic and anaerobic conditions at pH 2.0–12.0 are given in Tables 5 and 6. The results indicate that with an increase in RF concentration, the rate of photodegradation of PD also increases. The rates of degradation of PD in the presence of RF in aerobic and anaerobic conditions under UV and visible irradiation are in the range of 0.046–7.551 and 0.009–0.755 × 10^{-2} min^{-1}, respectively. In aerobic conditions, the photodegradation rates are 10-fold higher than those of anaerobic conditions (Tables 5 and 6). These higher rates of photodegradation of PD in the presence of RF in aerobic conditions are due to the PD degradation by two separate photosensitized degradation pathways (type I and II) as reported earlier.[63,79,80] The rate of RF sensitized photodegradation of PD is higher in aerobic conditions than in anaerobic conditions due to the oxygen involvement in the degradation process. This oxygen interacts with the excited state of RF, forming $^1O_2$ (singlet oxygen), O_2^- (super anion radicals) and $OH^•$ (hydroxy radicals). These species attack on the PD molecules resulting in a higher rate of photodegradation. However, in anaerobic conditions, the absence of oxygen retarded the formation of ROS which results in the slowdown of the rate of degradation of PD molecule. RF is known to photosensitize the degradation of drugs/substrates by both type I and II mechanisms.[70–73] In the present study, the degradation rate is 10-fold higher in aerobic conditions than in anaerobic conditions. So, therefore, we speculate that the higher RF-sensitized degradation in aerobic conditions is due to the PD following two different pathways (type I and II) for its degradation in the presence of RF as reported earlier.[63,79,80] RF sensitized photodegradation of different drugs ascorbic acid,[63,67,79,80] cyanocobalamin,[130–132] and folic acid[17] has previously been reported and found that RF catalyzes the photodegradation of these drugs.

The second-order rate (k_2) constants have been calculated to evaluate the effect of RF concentrations on the RF sensitized photodegradation of PD. The expression to calculate the k_2 for the RF sensitized photodegradation of PD is given below.

$$\text{Rate} = k_2[\text{PD}][\text{RF}] \quad (2)$$

where k_2 = second-order rate constants for the RF sensitized photodegradation of PD, [PD] = the concentration of PD (1.00 × 10^{-4} M), [RF] = the concentration of RF varies from 0.1–0.50 × 10^{-4} M to evaluate the effect of RF on the photodegradation of PD.

It has been found that with an increase in the concentration of RF, the rate of photodegradation increases indicating that RF acts as a sensitizer/promoter for the photodegradation of PD. The second-order (k_2) rate constant was calculated to evaluate the photochemical interaction between PD and RF (Tables 5 and 6) in aerobic and anaerobic conditions under UV and visible irradiation by plotting the values of k_{obs} *versus* RF concentration (0.05–0.5 × 10^{-4} M). These second-order plots for the photodegradation of PD in the presence of RF are given in Fig. S9 and S10† in aerobic and anaerobic conditions. It has been found that as the pH increases, the photodegradation rate of PD also increases in the presence of RF. The rates (k_0) of photodegradation of PD in the absence of RF in aerobic and anaerobic conditions using UV and visible irradiation are reported in Tables 5 and 6, respectively.

3.7 k_2–pH profile

The stability of liquid vitamin preparations is critical, and to achieve this, stability studies have been undertaken. The photochemical interaction of PD with the RF has been evaluated by plotting the second-order rate constants (k_2) *versus* pH (Fig. 9). The k_2–pH profile shows a slant curve which shows that with an increase in pH (2.0–12.0), the rate of photodegradation also increases in the presence of RF in aerobic and anaerobic conditions. PD in an aqueous solution shows four ionic forms that are interchangeable.[133] It is a dipolar molecule (pK_{a1} 5.0, pK_{a2} 9.0) due to which PD is present in distinct ionic species at acidic and alkaline pH. The type and conformation of these ionic species are based on the variations of acid–base equilibria in the whole pH range. Below pH 5.0, it is present in its cationic form, and at pH 6.8, it is present in its dipolar or neutral form. Whereas, at pH 8.0 and greater it is present in its anionic form.[134–136] These equilibria for the ionic species are given in Fig. 10. The different ionic species of PD (cationic, anionic, dipolar, neutral) are prone to photodegradation and the extent of photodegradation in the presence of RF in aerobic and

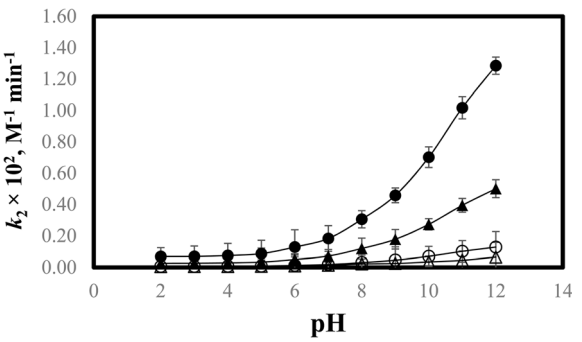

Fig. 9 k_2–pH profile for the photodegradation of PD in the presence of RF in aerobic and anaerobic conditions using UV and visible irradiation sources: aerobic visible (●) and UV (▲), anaerobic visible (○) and UV (Δ).

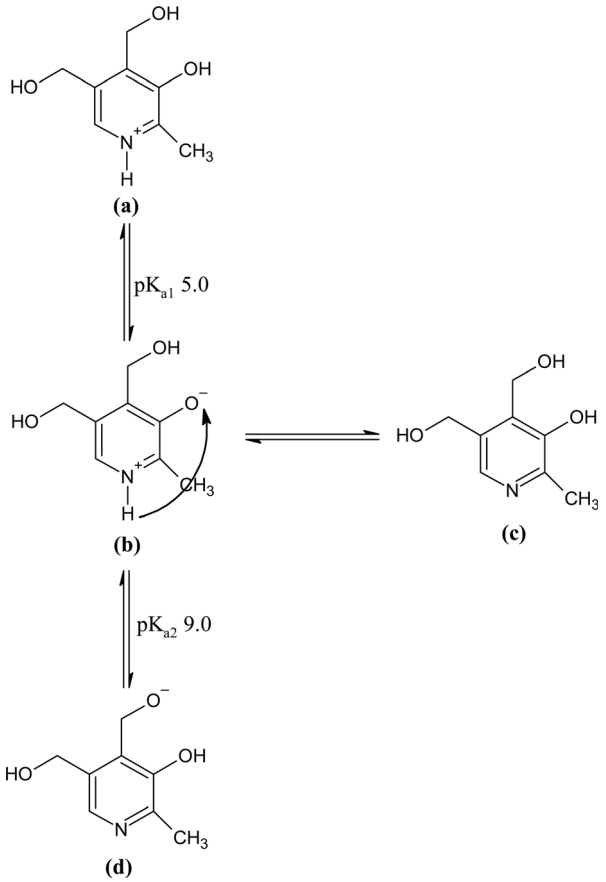

Fig. 10 Ionic species and tautomeric forms of PD in aqueous solution: (a) cationic (b) dipolar (c) neutral, and (d) anionic species.

anaerobic conditions is dependent on the sensitivity of the excited triplet state at a particular pH. When the drug (PD) molecule is solubilized in the aqueous solution (pH 2.0–12.0) resulting in the formation of various ionic (anionic and cationic) and neutral species. The rate of photodegradation of these PD species in the presence of RF is highly dependent on the specific ionizable form of PD at various pH. RF acts as a photosensitizer for the photodegradation of PD and could interact differently with the PD species at different pH enhancing or slowing down the rate of degradation of PD. The reactive oxygen species (ROS) produced in the presence of RF differently or variably interact with these ionizable forms of PD which increases (anionic species of PD) or decreases (cationic species of PD) the rate of photodegradation. It has been found that in the presence of RF, the cationic species are less susceptible to photodegradation as compared to the neutral, dipolar, and anionic species of PD. The photodecomposition rate of PD in the presence of RF slowly increased from pH 2.0 to 6.0, which may be due to the photochemical interaction of PD species (PDH^-) (pK_{a1} 5.0)[136] with RF in its deprotonated form. At pH 2.0–6.0, the ionized species range from 0.01–99.9%, respectively, which indicates that these species are susceptible to singlet oxygen ($^1O_2$) for their photodegradation in the presence of RF.

The decrease in the degradation rate at pH 2.0 in the presence of RF is due to the formation of inactive protonated RF (N-10) and oxonium cation.[49] The rate of photodegradation increases above pH 2.0 due to the pronounced susceptibility of PD ions in the presence of RF which in its non-ionized form is considerably stable at pH 4.0–6.0.[25,54,137] The rate of photodegradation in the presence of RF in aerobic and anaerobic conditions gradually increases from pH 7.0 to 8.0 and afterward from pH 9.0 to 12.0 (pK_{a2} 9.0), a fast increase in the photodegradation has been observed. At pH 9.0 to 12.0, the ionized species of PD vary from 50.0 to 99.9%, indicating that the anionic form of PD is more prone to RF-sensitized photodecomposition in comparison with that of the cationic form. The higher rate of degradation in this pH range is due to the pronounced interaction of non-ionized species of RF with PD.

3.8 Photolysis quantum yields

In aerobic and anaerobic conditions, the quantum yields of photolysis of PD in the presence of RF have been calculated and are given in Tables 5 and 6, respectively. These values were found to be in the range of 0.108–9.090 and 0.019–0.909 for aerobic and anaerobic conditions, respectively. The values obtained indicate the sensitivity of the excited triplet state during the photolysis reaction. The higher values of quantum yield of photolysis show the greater sensitivity of the excited triplet state towards photolytic degradation and *vice versa*.

3.9 TOC analysis

The mineralization of PD, RF, and RF–PD has been determined using the TOC analyzer, and the results obtained are given in Table 7. It has been found that the undegraded PD, RF, and RF–PD show higher TOC values, which on photolysis results in decreased TOC values, indicating the mineralization and

Table 7 TOC analysis of PD (1.00×10^{-4} M), RF (5.00×10^{-5} M) and RF–PD at pH 7.0 before and after visible irradiation. The values indicate the average of three separate determinations

	Before irradiation			After irradiation			
	TOC[a] (ppb) ± SD	IC[b] (ppb) ± SD	TC[c] (ppb) ± SD	TOC[a] (ppb) ± SD	IC[b] (ppb) ± SD	TC[c] (ppb) ± SD	Total TOC loss[d] (%)
PD	203 ± 0.92	621 ± 1.02	824 ± 0.56	43.5 ± 0.22	741 ± 0.76	784.5 ± 0.71	78.6
RF	270 ± 0.66	577 ± 1.00	847 ± 0.22	22.8 ± 0.55	611 ± 1.06	633.8 ± 0.88	91.6
RF-PD	651 ± 0.71	866 ± 0.54	1517 ± 0.32	356 ± 1.10	684 ± 0.87	1040 ± 0.51	45.3

[a] TOC = total organic carbon. [b] IC = inorganic carbon. [c] TC = total carbon. [d] Total TOC loss (%) = 100 − TOC.

increased degradation of these substances as reported earlier.[138,139] The TOC values are found to be significantly decreased, which indicates the degradation of PD, RF, and RF–PD, which may lead to the formation of smaller organic fragments, CO_2, and inorganic substances that result in the decreased TOC contents in the samples after photodegradation. The % loss of TOC after photolysis for PD, RF, and RF–PD are 78.6%, 91.56%, and 45.32%, respectively (Table 7).

3.10 Mode of photodegradation

The process of photodegradation for PD has been conducted in an aqueous solution (pH 2.0–12.0). The possible mechanism for the photodecomposition of PD in an aqueous solution is discussed below.

3.10.1 PD photodegradation in aqueous solution. PD when absorbed light is then converted into an excited singlet state (^{1}[PD]) (eqn (3)) which is subsequently converted into an excited triplet state (^{3}[PD]) (eqn (4)) *via* intersystem crossing (isc). This excited triplet state (^{3}[PD]) when interacting with the ground state (^{0}[PD]) leads to the formation of cationic ([PD$^{\bullet+}$]) and anionic radicals ([PD$^{\bullet-}$]) (eqn (5)) of PD. These cationic and anionic radicals accept or lose the H^+ atom resulting in the formation of oxidized (eqn (6)) and reduced (eqn (7)) radicals of PD. The two reduced radicals (PDH$^\bullet$) interact with each other to form oxidized and reduced PD molecules (eqn (8)). The oxidized PD$^\bullet$ molecules lead to the formation of degradation products of PD (eqn (9)).

$$^0[PD] \xrightarrow{h\nu} {}^1[PD] \quad (3)$$

$$^1[PD] \xrightarrow{isc} {}^3[PD] \quad (4)$$

$$^3[PD] + {}^0[PD] \rightarrow PD^{\bullet-} + PD^{\bullet+} \quad (5)$$

$$PD^{\bullet+} \xrightarrow{-H^+} PD^\bullet \quad (6)$$

$$PD^{\bullet-} \xrightarrow{H^+} PDH^\bullet \quad (7)$$

$$2PDH^\bullet \xrightarrow{-H^+} PD^\bullet + PDH_2 \quad (8)$$

$$PD^\bullet \xrightarrow{-H^+} \text{degradation products} \quad (9)$$

3.10.2 Mode of interaction of PD with RF. It has been observed that the rate at which PD degrades increases with higher concentrations of RF. Therefore, RF acts as a promotor for the photodegradation of PD. It has previously been reported that RF catalyzes both type I and II photosensitized oxidation of analytes.[63,140,141] In type I oxidation leads to the formation of radicals *via* the transfer of proton or electron in the transition state of RF and analytes. Whereas in the type II mechanism, the $^1O_2$ (singlet oxygen) is formed by an energy transfer from ^{3}[RF] (excited triplet state) to $^3O_2$ (molecular oxygen) resulting in the photooxidation of drugs. So, therefore, the proposed mechanisms for the photodegradation of PD in aerobic and anaerobic conditions with RF are described below.

3.10.3 Aerobic condition

3.10.3.1 Type I mechanism. RF is converted to its excited singlet state (^{1}[RF]) by absorbing light (eqn (10)), which is then converted into an excited triplet state (^{3}[RF]) through intersystem crossing (isc) (eqn (11)). This ^{3}[RF] afterward interacts with PDH^- ions to form PDH$^\bullet$ (eqn (12)). This PDH$^\bullet$ reacts with oxygen molecules to form PD (degradation products) and hydrogen peroxide (H_2O_2) (eqn (13)). So, therefore, RF enhances the photodegradation of PD.

$$^0[RF] \xrightarrow{h\nu} {}^1[RF] \quad (10)$$

$$^1[RF] \xrightarrow{isc} {}^3[RF] \quad (11)$$

$$^3[RF] + PDH^- \rightarrow RF^{-\bullet} + PDH^\bullet \quad (12)$$

$$PDH^\bullet + O_2 \rightarrow PD + H_2O_2 \quad (13)$$

3.10.3.2 Type II mechanism. RF is converted to its excited singlet state (^{1}[RF]) by absorbing light (eqn (14)), which is then converted into an excited triplet state (^{3}[RF]) *via* isc (eqn (15)). This excited triplet state (^{3}[RF]) reacts with molecular oxygen ($^3O_2$) and transforms into singlet oxygen ($^1O_2$) (eqn (16)). This $^1O_2$ afterward interacts with PDH and H^+ from the medium leading to the formation of degradation products (PD) and H_2O_2 (eqn (17)).

$$^0[RF] \xrightarrow{h\nu} {}^1[RF] \quad (14)$$

$$^1[RF] \xrightarrow{isc} {}^3[RF] \quad (15)$$

$$^3[RF] + {}^3O_2 \rightarrow {}^0[RF] + {}^1O_2 \quad (16)$$

$$PDH^- + {}^1O_2 + H^+ \rightarrow PD + H_2O_2 \quad (17)$$

3.10.4 Anaerobic condition. The ionized species (PDH^-) of PD react with ground state RF (^{0}[RF]) leading to the formation of ground state complex (^{0}[RF…PDH^-]) (eqn (18)), which is also confirmed by the *in silico* studies that RF forms a ground state complex with PD. This ^{0}[RF…PDH^-] absorb the light and transform it into an excited singlet state complex (^{1}[RF…PDH^-]) (eqn (19)). This ^{1}[RF…PDH^-] *via* isc converted into exciplex (^{3}[RF…PDH^-]) (excited triplet state complex) (eqn (20)).[142] The excited triplet state complex *via* H-abstraction from PDH^- to RF yields RFH$^\bullet$ (semiquinone radical)[59] and degradation products (PD) (eqn (21)). This semiquinone radical *via* disproportionation results in the formation of [RF_{OX}] (oxidized RF) and RFH_2 (reduced RF, dihydroriboflavin) (eqn (22)). The RFH_2 then reacts with $^3O_2$ (molecular oxygen) to form cationic RF radical ($RFH_2^{\bullet+}$) and anionic superoxide radical ($O_2^{\bullet-}$) (eqn (23)). Afterward, these two radicals recombine (radicals–radicals recombination) to form RF and H_2O_2 (eqn (24)). Also, the ^{3}[RF] interact with $^3O_2$ to form RF and $^1O_2$ (eqn (25)) and this $^1O_2$ may also transform into $^3O_2$ (eqn (26)).

$$^{0}[RF] + PDH^{-} \rightarrow \underset{\text{ground state complex}}{^{0}[RF\ldots PDH^{-}]} \quad (18)$$

$$^{0}[RF\ldots PDH^{-}] \xrightarrow{h\nu} {}^{1}[RF\ldots PDH^{-}] \quad (19)$$

$$^{1}[RF\ldots PDH^{-}] \xrightarrow{\text{isc}} \underset{\text{exciplex}}{^{3}[RF\ldots PDH^{-}]} \quad (20)$$

$$^{3}[RF\ldots PDH^{-}] \xrightarrow{\text{H-abstraction}} [RFH^{\cdot}] + PD \quad (21)$$

$$2RFH^{\cdot} \xrightarrow{\text{disproportionation}} RF_{ox} + RFH_2 \quad (22)$$

$$RFH_2 + {}^{3}O_2 \rightarrow RFH_2^{\cdot +} + O_2^{\cdot -} \quad (23)$$

$$RFH_2^{+} + O_2^{\cdot -} \xrightarrow{\text{radical-radical recombination}} RF + H_2O_2 \quad (24)$$

$$^{3}[RF] + {}^{3}O_2 \rightarrow {}^{0}[RF] + {}^{1}O_2 \quad (25)$$

$$^{1}O_2 \rightarrow {}^{3}O_2 \quad (26)$$

4. Conclusion

The present study aims to evaluate the role of riboflavin (RF) in photooxidative degradation of pyridoxine HCl (PD). RF increases the rate of photodegradation of PD and its rate of photodegradation is linearly dependent on the concentration of RF indicating that RF acts as a promoter for the PD degradation. The rate of degradation of PD increases with an increase in pH forming a slant curve with the maximum rate of photodegradation at pH 12.0 where the % ionization of PD is 99.90% indicating that the ionized form of PD is more susceptible to the RF-sensitized photooxidation. Two green analytical methods (UV-visible spectroscopic, high-performance liquid chromatographic methods) are developed and are effectively used for the simultaneous determination of PD and RF in pure and degraded solutions.

Data availability

Data will be available upon reasonable request to the corresponding author.

Conflicts of interest

Authors declare that there is no conflict of interest.

References

1 T. J. Macek, *Am. J. Pharm.*, 1960, **132**, 433–455.
2 E. R. Garrett, in *Advances in Pharmaceutical Sciences*, ed. Bean H. S., Beckett A. H. and Careless J. E., Academic Press, London, 1967, vol. 2, 1, pp. 1–94.
3 M. H. Hashmi, in *Assay of Vitamins in Pharmaceutical Preparations*, Wiley, New York, NY, 1973, vol. 2.
4 C. J. Litner, in *Quality Control in Pharmaceutical Industry*, ed. M. S. Cooper, Academic Press, New York, 1973, vol. 2, p. 185.
5 J. Kirschbaum, in *Analytical Profile of Drug Substances*, ed. K. Florey, Academic Press, New York, USA, 1981, vol. 10, pp. 183–288.
6 E. DeRitter, *J. Pharm. Sci.*, 1982, **71**, 1073–1096.
7 B. S. Yu, S. J. Lee, S. J. Lee and H. H. Chung, *J. Pharm. Sci.*, 1983, **72**, 592–596.
8 M. C. Allwood, *J. Clin. Pharm. Ther.*, 1984, **9**, 181–198.
9 I. Racz, *Drug Formulation*, Wiley, New York, 1989, pp. 121–122.
10 J. T. Carstensen, *Theory of Pharmaceutical Systems*, Academic Press, New York, 1972, pp. 211–214.
11 T. Ismail, *The Stability and Interaction of Hydroxocobalamine with Ascorbic Acid*, M. Phil. thesis, University of Karachi, 1995.
12 R. H. Shaikh, *Riboflavin Sensitized Photodegradation of Ascorbic Acid*, PhD thesis, University of Karachi, 1996.
13 H. H. Tonnesen, in *Photostability of Drug and Drugs Formulation*. Taylor & Francis, London, 1996, pp. 396–397.
14 H. H. Tonnesen, in *The Photostability of Drugs and Drug Formulations*, Culinary and Hospitality Industry Publications Services, Weimex, TX, 2004.
15 M. J. Akhtar, M. A. Khan and I. Ahmad, *J. Pharm. Biomed. Anal.*, 1997, **16**, 95–99.
16 M. J. Akhtar, M. A. Khan and I. Ahmad, *J. Pharm. Biomed. Anal.*, 1999, **19**, 269–275.
17 M. J. Akhtar, M. A. Khan and I. Ahmad, *J. Pharm. Biomed. Anal.*, 2000, **23**, 1039–1044.
18 M. J. Akhtar, M. A. Khan and I. Ahmad, *J. Pharm. Biomed. Anal.*, 2003, **31**, 579–588.
19 F. H. M. Vaid, *Photolysis and Interaction of Thiamine HCl with Riboflavin in Aqueous Solution*, PhD thesis, University of Karachi, 1997.
20 M. C. Allwood and M. C. J. Kearney, *Nutrition*, 1998, **14**, 697–706.
21 M. Ahmad, *A Study of Photochemical Interaction of Cyanocobalamine with Thiamine and Pyridoxine*. PhD thesis, University of Karachi, 2001.
22 I. A. Ansari. *Photolysis and Interactions of Cyanocobalamin with some B Vitamins and Ascorbic Acid in Parenteral Solutions*, PhD thesis, University of Karachi, 2002.
23 I. Ahmad and W. Hussain, *Pak. J. Pharm. Sci.*, 1993, **6**, 23–28.
24 I. Ahmad, W. Hussain and A. A. Fareedi, *J. Pharm. Biomed. Anal.*, 1992, **10**, 9–15.
25 I. Ahmad, I. A. Ansari and T. Ismail, *J. Pharm. Biomed. Anal.*, 2003, **31**, 369–374.
26 I. Ahmad, Q. Fasihullah, A. Noor, I. A. Ansari and Q. N. Ali, *Int. J. Pharm.*, 2004, **280**, 199–208.
27 I. Ahmad, Q. Fasihullah, F. H. M. Vaid and J. Photochem, *J. Photochem. Photobiol., B*, 2004, **75**, 13–20.
28 I. Ahmad, Z. Anwar, S. A. Ali, K. A. Hasan, M. A. Sheraz and S. Ahmed, *J. Photochem. Photobiol., B*, 2016, **157**, 113–119.

29 I. Ahmad, S. Ahmed, M. A. Sheraz, Z. Anwar, K. Qadeer, A. Noor and M. P. Evstigneev, *Sci. Pharm.*, 2015, **201**(84), 289–303.
30 I. Ahmad, Z. Anwar, S. Ahmed, M. A. Sheraz and S. U. R. Khattak, *J. Photochem. Photobiol., B*, 2017, **20**, 505–510.
31 I. Ahmad, Z. Anwar, M. A. Sheraz, S. Ahmed and S. U. Khattak, *Luminescence*, 2018, **33**, 1070–1080.
32 I. Ahmad, T. Mirza, Z. Anwar, M. A. Ejaz, M. A. Sheraz and S. Ahmed, *Spectrochim. Acta, Part A*, 2018, **205**, 540–550.
33 I. Ahmad, T. Mirza, Z. Anwar, S. Ahmed, M. A. Sheraz, M. A. Ejaz and S. H. Kazi, *J. Photochem. Photobiol., A*, 2019, **374**, 106–114.
34 S. Yoshioka and V. J. Stella, *Stability of Drugs and Dosage Forms*, Kluwer Academic/Plenum, Publishers, New York, 2000, ch. 2.
35 S. C. Sweetman, *Martindale: The Complete Drug Reference*, Pharmaceutical Press, London, 36th edn, electronic version, 2009.
36 P. J. Sinko, *Martin's Physical Pharmacy and Pharmaceutical Sciences*, Lippincott Williams & Wilkins, Philadelphia, USA, 5th edn, 2006, ch. 8, 15, 18.
37 S. W. Baertschi, in *Pharmaceutical Stability Testing to Support Global Markets*, ed. K. Huynh - Ba, Springer, New York, USA, 2010, pp. 107–116.
38 Z. Anwar and I. Ahmad, in *Advances in Medicine and Biology*, ed. L. V. Berhardt, Nova Science Publishers, USA, 2017, ch. 4.
39 British Pharmacopoeia, *Monograph on Riboflavin*, Her Majesty's Stationary Office, London, UK, 2024, electronic version.
40 *United States Pharmacopeia 30/National Formulary 25, Electronic Version*, United States Pharmacopeial Convention, Inc., Rockville, MD, 2024, electronic version.
41 C. Y. Ang, *J. AOAC Int.*, 1979, **62**, 1170–1173.
42 M. F. Chen, J. R. H. Worth Boyce and L. Triplett, *JPEN, J. Parenter. Enteral Nutr.*, 1983, **7**, 462–464.
43 M. J. O'Neil, *The Merck Index*, Merck & Co. Inc., Rahway, NJ, USA, 15th edn, 2013, electronic version.
44 D. W. Brousmiche and P. Wan, *J. Photochem. Photobiol., A*, 2002, **149**, 71–81.
45 A. Yamaji, Y. Fujii, Y. Kurata, N. Onishi N and E. Hiroaka, *J. Pharm. Sci. Technol., Jpn.*, 1980, **40**, 143–150.
46 P. C. Buxton, S. M. Conduit and J. Hathaway, *Br. J. Intravenous Ther.*, 1983, **4**, 5–12.
47 N. Mizuno, A. Fujiwara and E. Morita, *J. Pharm. Pharmacol.*, 1981, **33**, 373–376.
48 P. Bilski, M. Y. Li, M. Ehrenshaft, M. E. Daub and C. F. Chignell, *Photochem. Photobiol.*, 2000, **71**, 129–134.
49 P. F. Heelis, *Chem. Soc. Rev.*, 1982, **11**, 15–39.
50 E. Sikorska, I. Khmelinskii, A. Komasa, J. Koput, L. F. Ferreira, J. R. Herance, J. L. Bourdelande, S. L. Williams, D. R. Worrall, M. Insińska-Rak and M. Sikorski, *Chem. Phys.*, 2005, **314**, 239–247.
51 I. Ahmad, Q. Fasihullah and F. H. M. Vaid, *J. Photochem. Photobiol., B*, 2006, **82**, 21–27.
52 I. Ahmad, Q. Fasihullah and F. H. M. Vaid, *Photochem. Photobiol. Sci.*, 2006, **5**, 680–685.
53 M. Insińska-Rak, A. Golczak and M. Sikorski, *J. Phys. Chem. A*, 2012, **116**, 1199–1207.
54 I. Ahmad, Z. Anwar, S. Ahmed, M. A. Sheraz, R. Bano and A. Hafeez, *AAPS PharmSciTech*, 2015, **16**, 1122–1128.
55 F. H. Vaid, W. Gul, A. Faiyaz, Z. Anwar, M. A. Ejaz, S. Zahid and I. Ahmad, *J. Photochem. Photobiol., A*, 2019, **371**, 59–66.
56 W. Gul, F. H. Vaid, A. Faiyaz, Z. Anwar, A. Khurshid and I. Ahmad, *J. Photochem. Photobiol., A*, 2019, **376**, 22–31.
57 M. Insińska-Rak, D. Prukała, A. Golczak, E. Fornal and M. Sikorski, *J. Photochem. Photobiol., A*, 2020, **403**, 112837.
58 Z. Anwar, S. A. Ali, M. R. Shah, F. Ahmed, A. Ahmed, U. Ijaz, H. Afzal, S. Ahmed, M. A. Sheraz, M. Usmani and I. Ahmad, *J. Mol. Struct.*, 2023, **1289**, 135863.
59 I. Ahmad and G. Tollin, *Photochem. Photobiol.*, 1981, **34**, 441–445.
60 I. Ahmad, M. A. Cusanovich and G. Tollin, *Proc. Natl. Acad. Sci. U. S. A.*, 1981, **78**, 6724–6728.
61 I. Ahmad, M. A. Cusanovich and G. Tollin, *Biochemistry*, 1982, **21**, 3122–3128.
62 I. Ahmad, Q. Fasihullah and F. H. M. Vaid, *J. Photochem. Photobiol., B*, 2005, **78**, 229–234.
63 A. Noreen, Z. Anwar, M. A. Ejaz, M. Usmani, T. Khan, M. A. Sheraz, S. Ahmed, T. Mirza, A. Khurshid and I. Ahmad, *Spectrochim. Acta, Part A*, 2024, **309**, 123813.
64 G. E. Treadwell, W. L. Cairns and D. E. Metzler, *J. Chromatogr.*, 1968, **35**, 376–388.
65 E. C. Smith and D. E. Metzler, *J. Am. Chem. Soc.*, 1963, **85**, 3285–3288.
66 P. F. Heelis, B. J. Parsons, G. O. Phillips and J. F. McKellar, *Photochem. Photobiol.*, 1981, **33**, 7–13.
67 P. F. Heelis, in *Chemistry and Biochemistry of Flavoenzymes*, ed. F. Muller, CRC Press Inc., Boca Raton, FL, USA, 1991, pp. 171–193.
68 M. A. Sheraz, S. H. Kazi, S. Ahmed, Z. Anwar and I. Ahmad, *Beilstein J. Org. Chem.*, 2014, **10**, 1999–2012.
69 M. A. Sheraz, S. H. Kazi, S. Ahmed, T. Mirza, I. Ahmad and M. P. Evstigneev, *J. Photochem. Photobiol., A*, 2014, **273**, 17–22.
70 E. Silva, V. Ruckert, E. Lissi and E. Abuin, *J. Photochem. Photobiol., B*, 1991, **11**, 57–68.
71 E. Silva, R. Ugarte, A. Andrade and A. M. Edwards, *J. Photochem. Photobiol., B*, 1994, **23**, 43–48.
72 E. Silva, P. Barrias, E. Fuentes-Lemus, C. Tirapegui, A. Aspee, L. Carroll, M. J. Davies and C. Lopez-Alarcon, *Free Radical Biol. Med.*, 2019, **131**, 133–143.
73 C. Challier, D. O. Mártire, N. A. García and S. Criado, *J. Photochem. Photobiol., A*, 2017, **332**, 399–405.
74 D. I. Pattison, A. S. Rahmanto and M. J. Davies, *Photochem. Photobiol.*, 2012, **11**, 38–53.
75 A. Knowles and E. M. Roe, *Photochem. Photobiol.*, 1968, **7**, 421–436.
76 J. R. Plimmer and U. I. Klingebiel, *Science*, 1971, **174**, 407–408.
77 P. I. Joseph-Bravo, M. Findley and P. M. Newberne, *J. Toxicol. Environ. Health, Part A*, 1976, **1**, 353–376.

78 P. Meisel, I. Amon, H. Hüller and K. Jährig, *Neonatol*, 1980, **38**, 30–35.
79 F. Şahbaz and G. Somer, *Food Chem.*, 1993, **46**, 177–182.
80 M. Y. Jung, S. K. Kim and S. Y. Kim, *Food Chem.*, 1995, **53**, 397–403.
81 R. Shimizu, M. Yagi and A. Kikuchi, *J. Photochem. Photobiol. B Biol.*, 2019, **191**, 116–122.
82 A. Yoshimura and T. Ohno, *Photochem. Photobiol.*, 1988, **48**, 561–565.
83 J. N. Chacon, J. McLearie and R. S. Sinclair, *Photochem. Photobiol.*, 1988, **47**, 647–656.
84 E. D. Silva, *Biol. Res.*, 1996, **29**, 57–68.
85 J. Garcia and E. Silva, *J. Nutr. Biochem.*, 1997, **8**, 341–345.
86 H. W. Chan, *J. Am. Oil Chem. Soc.*, 1977, **54**, 100–104.
87 J. M. King and D. B. MIN, *J. Food Sci.*, 1998, **63**, 31–34.
88 E. Silva, T. González, A. M. Edwards and F. Zuloaga, *J. Nutr. Biochem.*, 1998, **9**, 149–154.
89 E. Silva, A. M. Edward and D. Pacheco, *J. Nutr. Biochem.*, 1999, **10**, 181–185.
90 A. Ramu, M. M. Mehta, J. Liu, I. Turyan and A. Aleksic, *Cancer Chemother. Pharmacol.*, 2000, **46**, 449–458.
91 C. Lu, W. Lin, W. Wang, Z. Han, S. Yao and N. Lin, *Phys. Chem. Chem. Phys.*, 2000, **3**, 329–334.
92 A. Posadaz, E. Sanchez, M. I. Gutierrez, M. Calderon, S. Bertolotti, M. A. Biasutti and N. A. Garcıa, *Dyes Pigm.*, 2000, **45**, 219–228.
93 A. Pajares, J. Gianotti, G. Stettler, S. Bertolotti, S. Criado, A. Posadaz, F. Amat-Guerri and N. A. García, *J. Photochem. Photobiol., A*, 2001, **139**, 199–204.
94 T. J. Dickerson, N. Yamamoto and K. D. Janda, *Bioorg. Med. Chem.*, 2004, **12**, 4981–4987.
95 W. A. Massad, S. Bertolotti and N. A. Garcia, *Photochem. Photobiol.*, 2004, **79**, 428–433.
96 W. A. Massad, J. M. Marioli and N. A. Garcia, *Pharmazie*, 2006, **61**, 1019–1021.
97 R. R. Yettella and D. B. Min, *J. Agric. Food Chem.*, 2008, **56**, 10887–10892.
98 D. O. Ha, M. K. Jeong, C. U. Park, M. H. Park, P. S. Chang and J. H. Lee, *J. Food Sci.*, 2009, **74**, 380–384.
99 A. Juzeniene, T. T. Thu Tam, V. Iani and J. Moan, *Free Radical Biol. Med.*, 2009, **47**, 1199–1204.
100 R. S. Scurachio, L. H. Skibsted, G. Metzker and D. R. Cardoso, *Photochem. Photobiol.*, 2011, **87**, 840–845.
101 M. P. Montaña, G. Ferrari, E. Gatica, J. Natera, W. Massad and N. A. García NA, *Can. J. Chem.*, 2013, **91**, 684–690.
102 J. M. Grippa, A. De Zawadzki, A. B. Grossi, L. H. Skibsted and D. R. Cardoso, *J. Agric. Food Chem.*, 2014, **62**, 1153–1158.
103 E. Reynoso, M. B. Spesia, N. A. García, M. A. Biasutti and S. Criado, *J. Photochem. Photobiol., B*, 2015, **142**, 35–42.
104 C. Gambetta, W. A. Massad, A. V. Nesci and N. A. García, *Pure Appl. Chem.*, 2015, **87**, 997–1010.
105 M. S. Díaz and M. M. Luiz, *Redox Rep.*, 2015, **20**, 17–25.
106 D. Cacciari, E. Reynoso, M. B. Spesia, S. Criado and M. A. Biasutti, *Redox Rep.*, 2017, **22**, 166–175.
107 J. Meng, F. Xu, S. Yuan, Y. Mu, W. Wang and Z. H. Hu, *J. Chem. Eng.*, 2019, **355**, 130–136.
108 A. Reynoso, D. Possetto, E. De Gerónimo, V. C. Aparicio, J. Natera and W. Massad, *J. Photochem. Photobiol., A*, 2021, **412**, 113213.
109 A. Pavanello, D. Fabbri, P. Calza, D. Battiston, M. A. Miranda and M. L. Marin, *J. Photochem. Photobiol., B*, 2021, **221**, 112250.
110 ICH Harmonized Tripartite Guideline, Validation of analytical procedures: text and methodology Q2 (R1), *Paper Presented at International Conference on Harmonization of Technical Requirements for Registration of Pharmaceuticals for Human Use*, Geneva, Switzerland, 2005.
111 I. Ahmad, H. D. C. Rapson, P. F. Heelis and G. O. Phillips, *J. Org. Chem.*, 1980, **45**, 731–733.
112 T. R. Watkins, A. Smith and J. C. Touchstone, *J. Chromatogr.*, 1986, **374**, 221–222.
113 C. G. Hatchard and C. A. Parker, *Proc. R. Soc. London, Ser. A*, 1956, **235**, 518–536.
114 I. Ahmad, T. Mirza, S. G. Musharraf, Z. Anwar, M. A. Sheraz, S. Ahmed, M. A. Ejaz and A. Khurshid, *RSC Adv.*, 2019, **9**, 26559–26571.
115 A. Khurshid, I. Ahmad, N. Khan, M. Usmani and Z. Anwar, *Int. J. Chem. Kinet.*, 2023, **55**, 190–203.
116 M. Srivastava, P. Rani, N. P. Sing and R. A. Yadav, *Spectrochim. Acta, Part A*, 2014, **120**, 274–286.
117 R. Padmavathi, S. Gunasekaran and B. Rajamannan, *Int. J. Sci. Res.*, 2017, **7**, 1146–1160.
118 A. C. Talari, M. A. Martinez, Z. Movasaghi, S. Rehman and I. U. Rehman, *Appl. Spectrosc. Rev.*, 2017, **52**, 456–506.
119 K. Sugibayashi, Y. Yoshida, R. Suzuki, K. Yoshizawa, K. Mori, S. Itakura, K. Takayama and H. Todo, *Pharmaceutics*, 2020, **12**, 427.
120 C. M. Harris, R. J. Johnson and D. E. Metzler, *Biochim. Biophys. Acta, Gen. Subj.*, 1976, **421**, 181–194.
121 M. Ristilä, J. M. Matxain, Å. Strid and L. A. Eriksson, *J. Phys. Chem. B*, 2006, **110**, 16774–16780.
122 M. S. Imam and M. M. Abdelrahman, *Trends Environ. Anal. Chem.*, 2023, e00202.
123 M. Locatelli, A. Kabir, M. Perrucci, S. Ulusoy, H. I. Ulusoy and I. Ali, *Advances in Sample Preparation*, 2023, 100068.
124 C. Furió-Sanz, D. Gallart-Mateu, S. Armenta, S. Garrigues and M. de la Guardia, *Talanta Open*, 2023, **7**, 100195.
125 L. P. Kowtharapu, N. K. Katari, S. K. Muchakayala and V. M. Marisetti, *TrAC, Trends Anal. Chem.*, 2023, **166**, 117196.
126 L. Persson, S. Karlsson-Vinkhuyzen, A. Lai, Å. Persson and S. Fick, *Sustainability*, 2017, **9**, 2176.
127 J. Płotka-Wasylka and W. Wojnowski, *Green Chem.*, 2021, **23**, 8657–8665.
128 J. Płotka-Wasylka, *Talanta*, 2018, **181**, 204–209.
129 F. Pena-Pereira, W. Wojnowski and M. Tobiszewski, *Anal. Chem.*, 2020, **92**, 10076–10082.
130 A. R. Rogers and J. A. Yacomeni, *J. Pharm. Pharmacol.*, 1971, **23**, 218S.
131 I. A. Ansari, F. H. M. Vaid and I. Ahmad, *Pak. J. Pharm. Sci.*, 2004, **17**, 19–24.
132 I. A. Ansari, F. H. M. Vaid and I. Ahmad, *Pak. J. Pharm. Sci.*, 2004, **17**, 83–93.

133 D. E. Metzler and E. E. Snell, *J. Am. Chem. Soc.*, 1955, **77**, 2431–2437.
134 R. L. Gustafson and A. E. Martell, *Arch. Biochem. Biophys.*, 1957, **68**, 485–498.
135 Y. Matsushima and A. E. Martell, *J. Am. Chem. Soc.*, 1967, **89**, 1322–1330.
136 M. S. Refat, H. M. Al-Maydama, F. M. Al-Azab, R. R. Amin and Y. M. Jamil, *J. Photochem. Photobiol., A*, 2014, **128**, 427–446.
137 B. Allard, H. Boren, C. Pettersson and G. Zhang, *Environ. Int.*, 1994, **20**, 97–101.
138 M. Perez-Moya, T. Kaisto, M. Navarro and L. J. Del Valle, *Environ. Sci. Pollut. Res. Int.*, 2017, **24**, 6241–6251.
139 W. L. Cairns and D. E. Metzler, *J. Am. Chem. Soc.*, 1971, **93**, 2772–2777.
140 G. R. Buettner and M. J. Need, *Cancer Lett.*, 1985, **25**, 297–304.
141 D. B. Min, *Presented at International Seminar, The Recent Status and Prospective in Agricultural Research*, Deajeon, Korea, 1991, pp. 18–23.
142 A. Knowles and G. N. Mautner, *Photochem. Photobiol.*, 1972, **15**, 199–207.